TRIM25 controls the Androgen Receptor and PSA/KLK3 levels in Prostate Cancer

Zur Erlangung des akademischen Grades einer

DOKTORIN DER NATURWISSENSCHAFTEN
(Dr. rer. nat.)

von der KIT-Fakultät für
Chemie und Biowissenschaften
des Karlsruher Instituts für Technologie (KIT)

genehmigte

DISSERTATION

von

M.Sc. Eleonora Pauletto
geb. in San Vito al Tagliamento, Italien

Hauptreferent:	Priv. Doz. Dr. rer. nat. Christine Blattner
Korreferent:	Prof. Dr. rer. nat. Andrew Cato

Zusammenfassung

Prostatakrebs ist eine häufig auftretende bösartige Erkrankung, die durch eine Abhängigkeit vom Androgenrezeptor (AR) gekennzeichnet ist. Obwohl es inzwischen verschiedene Therapien gibt, besteht weiterhin Bedarf, neue regulatorische Mechanismen der AR-abhängigen Signaltransduktion zu erforschen und potenzielle therapeutische Zielmoleküle zu identifizieren.
In dieser Studie wurde die Funktion von TRIM25 bei Prostatakarzinomzellen untersucht, einem Protein, das wir zuvor als Regulator von p300 identifiziert haben. p300 ist ein wichtiger Regulator des AR. Unsere bisherigen Ergebnisse zeigen, dass TRIM25dass TRIM25 den Abbau von p300 fördert. Wir vermuteten deshalb, dass TRIM25 die AR-Aktivität über die Regulation von p300 modulieren könnte.
Mittels RNA-Sequenzierungsanalyse wurde nachgewiesen, dass die genetische Entfernung von TRIM25 zu einer erhöhten AR-Aktivität führt, die zum Beispiel durch die Induktion von KLK3 und TMPRSS2, zwei wichtigen Zielgenen des AR, belegt ist. Zusätzlich zeigte die Analyse von Prostatakarzinomzellen mittels Massenspektrometrie erhöhte Mengen des KLK3 Proteins in TRIM25-Knockout-Zellen, was ebenfalls eine Modulation der AR-Aktivität durch TRIM25 belegt.
Interessanterweise wurde beobachtet, dass die genetische Entfernung von TRIM25 die Expression von KLK3 auch in Abwesenheit von Androgenen erhöhte.
Um die Mechanismen herauszufinden, die der TRIM25-vermittelten Modulation der AR-Aktivität zugrunde liegen, wurde untersucht, ob TRIM25 die Menge des AR oder seine subzelluläre Lokalisation beeinflussen könnte. Das war jedoch nicht der Fall. TRIM25 verstärkte jedoch die Bindung des AR an den Enhancer-Bereich von KLK3.
Interessanterweise blockierte die Behandlung von Prostatakarzinomzellen mit, einem Inhibitor von p300, die verstärkte Transkription von KLK3 in Abwesenheit

von TRIM25, was die Bedeutung von p300 bei der TRIM25-vermittelten Modulation der AR-Aktivität unterstreicht.
Im Einklang mit der verstärkten Aktivität des AR und der erhöhten KLK3 Proteinmenge war auch die Zellproliferation in Abwesenheit von TRIM25 erhöhte.
Zusammenfassend zeigen diese Ergebnisse, dass TRIM25 die Aktivität des AR beeinflussen kann. Damit könnte TRIM25 ein therapeutisches Zielprotein zur Modulation der der AR-Aktivität bieten und zur Entwicklung neuer Behandlungsmethoden für Prostatakrebs beitragen.

Abstract

Prostate cancer is a prevalent malignancy characterized by the dependency on androgen receptor (AR) activity for growth and progression. While various therapies targeting AR have been developed, there is still a need to explore novel regulatory mechanisms regulating AR activity and to identify potential therapeutic targets.
In this study, the role of TRIM25 in prostate cancer was investigated. TRIM25 is a protein that we previously found to regulate p300, a crucial regulator of AR. Our previous findings revealed that TRIM25 promotes p300 degradation. Based on this, it was hypothesized that TRIM25 may modulate AR activity through the regulation of p300.
Using RNA-sequencing analysis, it was found that knockout of TRIM25 resulted in increased AR activity, as evidenced by the upregulation of *KLK3* and *TMPRSS2*, two key targets of AR. Additionally, mass spectrometry analysis revealed elevated levels of KLK3 protein in TRIM25 knockout cells, further supporting the role of TRIM25 in modulating AR activity.
Interestingly, TRIM25 knockout could modulate KLK3 expression even in the absence of androgens, suggesting both androgen-dependent and androgen-independent effects of TRIM25.
To elucidate the mechanisms underlying TRIM25-mediated modulation of AR activity, various aspects of AR function were examined. TRIM25 was found not to affect AR protein levels or its subcellular localization. Knocking out TRIM25, however, enhanced the binding of AR to the enhancer region of *KLK3*.
Moreover, it was discovered that TRIM25 exerts its effect on AR activity through p300. Inhibition of p300 effectively reduced the increased transcription of *KLK3* when TRIM25 was knocked out.
Finally, TRIM25 knockdown was observed to increase cell proliferation, which is consistent with the enhanced AR activity and elevated levels of KLK3.

In conclusion, these findings provide insights into the regulatory role of TRIM25 for AR activity in prostate cancer. Targeting TRIM25 and its interactions with p300 may hold therapeutic potential for modulating AR activity and could lead to the development of novel treatments for prostate cancer.

Contents

List of Abbreviations

ADT	androgen deprivation therapy
AR	androgen receptor
ARE	androgen response element
BPH	benign prostate hyperplasia
BSA	bovine serum albumin
CBP	CREB binding protein
CSS	charcoal-stripped bovine serum
cDNA	complementary DNA
ChIP	chromatin immunoprecipitation
CPM	counts per million
CRPC	castration-resistant prostate cancer
DBD	DNA binding domain
DHT	dihydrotestosterone
DMEM	Dulbecco's Modified Eagle Medium
DMSO	dimethyl sulfoxide
EtOH	ethanol
GSEA	Gene Set Enrichment Analysis
HAT	histone acetyltransferase
HDAC	histone deacetylase
kb	kilobases
kDa	kilodalton
KLK3	kallikrein-related peptidase 3
LBD	ligand binding domain
NCoR	nuclear receptor corepressor
NTD	N-terminal domain

OD	optical density
PCA	principal component analysis
PCa	prostate cancer
PSA	prostate specific antigen
RPMI	Roswell Park Memorial Institute 1640 Medium
RT-qPCR	quantitative real time PCR
SDS-PAGE	sodium dodecyl sulfate polyacrylamide gel electrophoresis
shRNA	short hairpin RNA
siRNA	small interfering RNA
SRC	steroid receptor coactivator
TIP60	Tat interactive protein 60
TMPRSS2	transmembrane protease, serine 2
TRIM	tripartite motif
TSS	transcription start site
vsd	variance-stabilized data
VST	variance stabilizing transformation

1 Introduction

1.1 Prostate cancer

Prostate cancer (PCa) is one of the most common cancers worldwide, being the most diagnosed type of cancer in men aged over 60 years old (Sung et al. 2021). In Germany, PCa accounted for 68,579 cases and 15,040 deaths in 2019 (Robert Koch Institute 2022).
PCa is uncommon in individuals under the age of 50 and its incidence increases with age. Age represents therefore an important risk factor. Although the understanding of other risk factors remains nowadays elusive, it seems that genetics and life-style can contribute to the development of PCa. The presence of other diseases may also increase the risk of PCa, including chronic inflammation of the prostate and sexually transmitted diseases (National Cancer Institute 2023).

The prostate is a walnut-shaped gland that sits below the urinary bladder in men. It is part of the male reproductive system as it produces and stores part of the seminal fluid. The prostate gland is separated into lobules by connective tissue. Each lobule consists itself of two main cell types, basal and luminal secretory cells, arranged in layers and surrounded by stroma (Bostwick & Cheng 2014). In normal prostate and in high grade prostate intraepithelial neoplasia (HGPIN), cell proliferation is confined to the epithelium. Although it is not clear if HGPIN will eventually develop into PCa, it is often considered to be a pre-malignancy. The most common type of PCa is adenocarcinoma, which develops when gland cells multiply abnormally and invade the surrounding stroma with generation of multifocal accumulations. Here, the tumour may invade nearby organs and spread to the lymph nodes and distant organs, such as bones, liver, and lungs (Cancer Research UK 2023).

1.1.1 Castration-resistant prostate cancer

Generally, both prostate gland cells and PCa cells are highly reliant on androgens, the male steroid hormones (Burris & McCabe 2000). In line with this, when tumours originate from prostatic epithelial cells, the prevailing clinical approach involves employing the androgen deprivation therapy (ADT). This therapeutic strategy aims to either diminish androgen levels or counteract the activation of the androgen receptor (AR). Although the ADT initially results in a positive clinical response, the majority of the patients experience tumour recurrence within 2-3 years (Harris et al. 2009). During this time, PCa develops into a more aggressive and hormone-independent form, which is referred to as castration-resistant PCa (CRPC). Interestingly, even during this hormone-independent stages, the AR signalling still plays a major role in PCa growth (Chandrasekar et al. 2015).
The majority of the mechanisms that have been proposed to explain the progression of PCa from a hormone-sensitive to a castration-resistant form are mediated by the AR. Some of the suggested mechanisms are (i) hypersensitivity to low androgen levels, through *AR* gene amplification (Visakorpi et al. 1995), or *AR* mutations (Gregory et al. 2001); (ii) disregulation of AR coactivators (Ueda et al. 2002, Debes et al. 2002); (iii) ligand-independent activation of AR by growth factors, cytokines and kinase pathways (Wang et al. 2009); (iv) altered androgen production (Sharifi 2013); (v) expression of AR variants (Dehm et al. 2008).

1.2 Androgen receptor

Like Dr. Huggings and his colleague Dr. Hodges had already published in the landmark study of PCa research in 1941, androgens, such as testosterone and its derivative dihydrotestosterone (DHT), mediate their tumour-promoting effects via the interaction with their receptor, the AR, and consequent activation of the AR signalling pathway (Huggins et al. 1941). As a matter of fact, the AR plays a crucial role in the development and advancement of PCa and is therefore a primary target for PCa treatment.

1.2.1 Androgen receptor structure

The AR is a steroid hormone nuclear receptor, whose gene is located on the X chromosome and is expressed in several tissues, including prostate, bone, muscle, adipose tissue, and the cardiovascular, neural and immune systems (Ruizeveld de Winter et al. 1991).
The *AR* gene encodes for a 110-kDa protein that consists of 919 amino acid residues. Like all steroid hormone receptors, the AR comprises four functional domains: the N-terminal domain (NTD), responsible for the transactivation function, the DNA binding domain (DBD), the ligand binding domain (LBD) and a flexible hinge region that connects the DBD to the LBD (MacLean et al. 1997). The NTD is the most variable region and can be therefore considered receptor-specific. On the contrary, the DBD and LBD are conserved regions between the different members of the steroid hormone receptor family (Ruizeveld de Winter et al. 1991). The DBD is formed by two zinc fingers that recognise specific DNA sequences called androgen responsive elements (AREs) on promoter and enhancer regions of AR-regulated genes. The direct binding of the AR to such sequences enables the activation functions of the NTD and LDB to either stimulate or repress the transcription of these genes. The function of the N-terminal LBD of the AR is to bind ligands, as well as to interact with heat shock proteins and coactivators (Claessens et al. 2008, Tan et al. 2014).
Other important features of the AR are its signal sequences. Two transcriptional activation domains have been identified within the AR, namely the activation function 1 and 2 (AF-1 and AF-2). The AF-1 is located in the NTD. It is required for its maximal activity and plays a crucial role in the ligand-independent transactivation of the AR (Lavery & McEwan 2006). The AF-2, located in the LBD, is responsible for the ligand-dependent transactivation of the receptor, whilst also mediating the interactions between the N-terminal and the ligand binding domains (C/N interactions). The conformational changes that this region is subjected to are important for forming the coregulator binding sites. Key differences in the AR AF-2 compared to the other nuclear receptors account for differences in their function, as well as the coregulatory proteins they interact with (He et al. 1999).

1.2.2 Androgen receptor action

The AR is involved in the differentiation and maturation of the male genitalia and is required for the development and maintenance of normal male sexual function (Quigley et al. 1992). Dysregulation of AR signalling can lead to a range of pathologies, including androgen insensitivity syndrome (AIS), spinal and bulbar muscular atrophy (SBMA), polycystic ovary syndrome (PCOS), breast cancer, benign prostatic hyperplasia (BPH), PCa (Shukla et al. 2016).
In the absence of hormone, the AR is a cytoplasmic protein associated with heat shock proteins and other chaperones. In this complex, the AR is protected from degradation and maintained in an appropriate conformation for ligand binding (Fang et al. 1996). When testosterone and, with higher affinity (Wilbert et al. 1983), DHT bind to the LBD of AR, conformational changes occur on the AF-2 that induce dissociation of AR from the cytoplasmic complex, AR phosphorylation, intramolecular interaction of the N- and C-terminal regions and exposure of the nuclear localisation signal (NLS) (Doesburg et al. 1997, Chen et al. 2012, Nazareth & Weigel 1996). As a result, the AR translocates into the nucleus through binding to importin-α (Kaku et al. 2008). In the nucleus, the AR dimerizes and binds to AREs in promoter or enhancer regions of its target genes (Heinlein & Chang 2004). The consensus ARE consists of two imperfect palindromic 6-bp elements separated by a 3-bp spacer: GG(A/T)ACAnnnTGTTCT (Roche et al. 1992). This type of binding site can also be recognised by other nuclear receptors, such as the glucocorticoid, progesterone and mineralcorticoid receptors. Nevertheless, besides this consensus ARE, other AR-specific binding sites have been identified for typical AR-target genes (Adler et al. 1993, Rundlett & Miesfeld 1995). Binding to the DNA allows the interaction of the AR with the transcriptional machinery to regulate gene transcription. Besides binding to the basal transcription factors, specific factors known as coregulators interact with the AR to either enhance (coactivators) or suppress (corepressors) its activity (Heinlein & Chang 2002) (Figure 1.1).

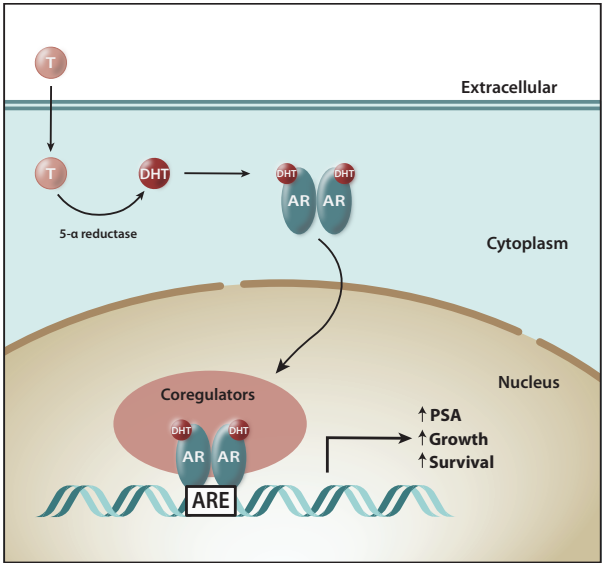

Figure 1.1: Androgen receptor action. The androgen receptor (AR) is a cytoplasmic protein that is activated by its ligand dihydrotestosterone (DHT), a metabolite of testosterone (T). Once activated, it translocates into the nucleus, dimerizes and binds to the androgen responsive elements (AREs) upstream of its target genes. Helped by a plethora of coregulators, the AR controls the transcription of several genes, promoting cell proliferation, tumour growth and increase of prostate specific antigen (PSA) levels.

1.2.3 Targeting the AR for prostate cancer therapy

An early-detection program under which eligible men can request a PSA (prostate specific antigen) test is an important part of an active surveillance strategy to detect PCa. PSA is the most widely used biomarker for PCa diagnosis, while being used for cancer recurrence and aggressiveness as well (Duffy 2020). Increasing levels of PSA in the blood of patients do not represent, however, proof of disease. To confirm the presence of a malignant tumour in the prostate, other tests are recommended to the patients, including the digital rectal examination, magnetic resonance imaging and tissue biopsies (Duffy 2020, Litwin & Tan 2017).
Once the patient has been diagnosed with PCa, the choice of treatment is based on different clinicopathological factors, including PSA concentrations and Gleason

score classification. For low-risk or intermediate-risk patients, active surveillance that allows monitoring of progression to a higher-risk tumour may be sufficient (Sandhu et al. 2021). For other patients, though, prostatectomy and/or radiotherapy may be the choice of treatment to cure the disease (Mottet et al. 2017). Patients with localized or metastatic high-risk PCa will be treated with radiotherapy alone or with hormonal therapy (ADT), whilst CRPCs can only be treated with chemotherapy (Golabek et al. 2016, Gravis et al. 2017).

ADT aims at achieving maximum androgen blockade with reduction of testosterone levels, in order to slow tumour progression (Evans 2018). This medical castration can be a result of drugs that block the synthesis of testosterone, or block the AR. The list of agents that block the AR includes enzalutamide (Furr et al. 1987, Evans 2018). Enzalutamide, one of the most studied AR antagonists, targets several steps in the AR signalling pathway (Clegg et al. 2012). This compound binds to the receptor with increased affinity compared to natural hormones. As a result, AR is prevented from translocating into the nucleus. Therefore, DNA binding of the AR does not occur and PSA levels are decreased (Scher et al. 2010). Enzalutamide distinguishes itself from other drugs by showcasing not just a delay in tumour growth but also the regression of tumours in mice (Tran et al. 2009). Although enzalutamide significantly decreases the risk of death among PCa patients, resistance inevitably develops in up to 46% of these patients (Scher et al. 2012, Beer et al. 2014).

Options for advanced androgen-independent PCa are chemotherapy with docetaxel and cabazitaxel, and immunotherapy (Evans 2018). However, these therapies are typically responsible for major side effects and only extend the patient's life by a few months (Tannock et al. 2004).

In light of these limitations, there is a pressing need for innovative strategies for the treatment of PCa.

1.3 Prostate specific antigen

1.3.1 PSA in clinics and in molecular biology

KLK3, also known as PSA, is the acronym for kallikrein related peptidase 3, a member of the kallikrein family. To ensure clarity and consistency, the gene and its corresponding protein will be consistently referred to as KLK3 in the following sections of this thesis.
The *KLK3* gene is located in chromosome 19 and is part of a locus that includes 14 other kallikrein genes. This cluster is the largest continuos cluster of peptidases in humans, spanning approximately 265 kb (Paliouras & Diamandis 2006).
Kallikreins are a subclass of serine proteases that have diverse physiological functions and have also been implicated in carcinogenesis (Borgono et al. 2004). KLK3 is synthesised in the epithelial cells of the prostate gland and from there secreted to form part of the seminal plasma (Lilja et al. 1985). Physiologically, its function is to hydrolyse high molecular weight proteins to liquefy the semen to have motile spermatozoa (Lilja et al. 1985). In the clinical setting, KLK3 is used to diagnose and monitor PCa in patients, as high levels of this protein in the blood have been correlated to higher risk of PCa. However, high levels of KLK3 in the blood of adult men can also be a consequence of other conditions, such as enlarged prostate, prostatitis or BPH (Stenman et al. 1998). Hence, the results of the KLK3 test can be misleading and have to be supported by other means.

Beyond its role as a biomarker, KLK3 has been shown to have an impact on several signalling pathways, including cell proliferation, angiogenesis and metastasis. For example, KLK3 can cleave a number of IGF (insulin growth factor) binding proteins, with consequent release of IGFs (Réhault et al. 2001). These proteins have been implicated in several types of cancers, including PCa, as proliferative factors, and can therefore cause tumour growth (Shim & Cohen 1999). Interestingly, KLK3 can induce cell proliferation by affecting the AR transactivation. In specific, it was shown that increased KLK3 levels could modulate the p53 pathway, which resulted in enhanced ARA70 (androgen receptor activator 70)-induced AR transactivation. This led to a decrease in apoptosis and an increase in cell

proliferation in PCa cells (Niu et al. 2008).
Several studies have furthermore shown a key role of KLK3 in the epithelial to mesenchymal transition (EMT). For example, KLK3 was reported to cleave proteins like collagen type IV (Pezzato et al. 2004), fibronectin and laminin (Webber et al. 1995), and activate other enzymes involved in EMT, such as the pro-MMP2 (metalloproteinase-2) (Veveris-Lowe et al. 2005). Furthermore, KLK3 can activate trypsin and granzyme B, extracellular proteases that can cleave extracellular matrix proteins. This leads to a degradation of the extracellular matrix and death of PCa cells in vitro (Rogers et al. 2018). KLK3 also has the potential of upregulating osteoblastic markers and it was hypothesised to be associated with osteoblastic phenotype of bone metastasis (Cumming et al. 2011).
Finally, KLK3 has also been shown to control angiogenesis in vitro, although it is not clear whether it has a favourable or unfavourable effect. It is suggested that its function may vary depending on the tumour context and availability of the substrates (Heidtmann et al. 1999, Jha et al. 2019).
As knowledge about the role of KLK3 in PCa progression has grown, there has been increasing interest in targeting KLK3 in PCa, as downregulation of its activity could represent an attractive therapeutic approach (Moradi et al. 2019).

1.3.2 Transcriptional control of PSA by the AR

As stated above, the AR controls *KLK3* expression as a result of its activation and binding to the AREs upstream of the *KLK3* gene.
The AR binds to several sites upstream of the *KLK3* gene. The first *KLK3* ARE (AREI) was identified in 1991 by Riegman and colleagues, on the promoter of the gene, at −170 to −156 bp from the transcription start site (TSS) (Riegman et al. 1991). The second ARE, AREII, was identified at −400 bp from the TSS and reported to have low affinity for AR and to cooperate with AREI (Cleutjens et al. 1996). AREI and II are considered unspecific, as they are active not only in PCa cell lines, but also in others, such as pancreatic (Panc-1) and ovarian (Ovcar-3) cancer cell lines (Schuur et al. 1996). Conversely, *KLK3* expression is specifically regulated in PCa cells by an upstream enhancer that includes the AREIII and that is located farther from the TSS, between −5824 and −3738 bp from the TSS (Schuur

et al. 1996). This region was later discovered to contain AREs IIIA, IIIB, IV, V, and VI and, although these sequences do not contain consensus ARE motifs, they can bind recombinant AR and contribute significantly to the androgen-dependent transcriptional activity (Huang et al. 1999). The distant AREs present in the *KLK3* promoter and enhancer regions may be brought together by chromatin looping to form a transcription complex with other factors, where the AR binds to both regions. This allows a synergic control of DNA transcription (Shang et al. 2002) (Figure 1.2).

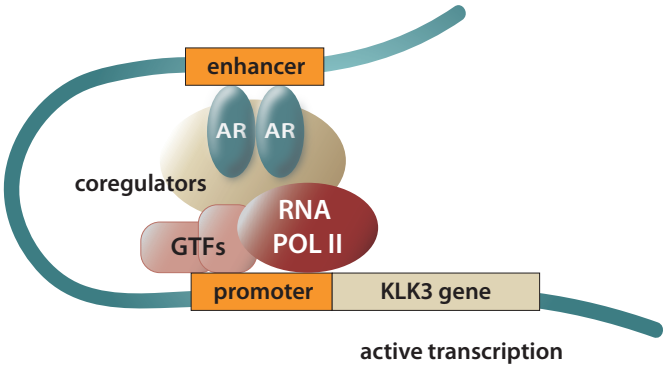

Figure 1.2: Representation of the molecular interactions and regulation at the *KLK3* locus. The androgen receptor (AR) binds to the enhancer region of *KLK3*, while RNA polymerase II (RNA pol II) binds to the promoter region. Chromatin looping facilitates the interaction between the enhancer and promoter, enabling the transcriptional activation of the *KLK3* gene. Additionally, general transcription factors (GTFs) and coregulators of AR contribute to the finely tuned regulation of gene expression.

1.4 AR coregulators

Binding of AR to its binding sites on the DNA profoundly depends on coactivators and corepressors. These coregulators can act with different mechanisms. They can affect the stability, ligand binding and cellular localization of AR. Otherwise, coactivators can bridge DNA-bound AR and general transcription factors, or modify chromatin to make promoters more or less accessible (Heinlein & Chang

2002).
Among the coregulators that inhibit the AR is the nuclear receptor corepressor (NCoR). Through its interaction with AR, NCoR effectively suppresses the transcriptional activity of AR (Hodgson et al. 2005). NCoR also recruits histone deacetylases (HDACs) to AR target gene promoters, leading to the deacetylation of histones, and thus to reduced accessibility of chromatin and to gene repression (Guenther et al. 2001).
Prominent AR coactivators are the p160 family of proteins, which include the steroid receptor coactivators SRC-1, SRC-2, and SRC-3. These coregulators enhance the AR-mediated transcription by either acetylating histones and thus promote accessible chromatin structure, or by interacting with the LBD and NTD of the AR (Bevan et al. 1999, Nakka et al. 2013, Irvine et al. 2000). Moreover, SRCs can enhance the AR activity by recruiting other proteins involved in chromatin remodelling and facilitating the assembly of transcriptional complexes. In specific, they can recruit ATP-dependent chromatin remodeling complexes, such as SWI/SNF, and coactivators with histone acetyltransferase (HAT) activity, including PCAF (p300/CBP-associated factor), TIP60 (Tat interactive protein 60) and p300/CBP (Spencer et al. 1997, Leo & Chen 2000).

Other essential coregulators of th AR are p300 and its homologous CBP (CREB binding protein). p300/CBP is a protein that acts as a bridge between transcription factors and the basal transcriptional machinery, facilitating the recruitment of transcriptional machinery to specific gene promoters (Cho et al. 1998, Nakajima et al. 1997). p300 modulates AR transcriptional activity by facilitating the assembly of coactivator complexes and chromatin remodelling complexes (Shang et al. 2002). It interacts with the AR through its bromodomain, which recognizes acetylated lysine residues, leading to the formation of a transcriptionally active complex (Aarnisalo et al. 1998, Yu et al. 2020). Apart from its HAT activity, p300 can also acetylate lysine residues of non-histone proteins, including the AR. By doing so, p300 increases the transcriptional activity of the AR (Fu et al. 2000). Moreover, p300 enhances AR stability by inhibiting its degradation, thereby amplifying the AR-mediated transcriptional output (Zhong et al. 2014). The aberrant expression or dysregulation of p300 has been observed in PCa, where it contributes to the uncontrolled growth and progression of tumour cells. The p300 inhibitor CCS1477

has demonstrated efficacy in reducing tumour growth both in vitro and in vivo. Currently, it is undergoing phase 1/2 of clinical trials for advanced PCa, indicating the potential of p300 as a therapeutic target (Welti et al. 2021).

1.5 TRIM25

1.5.1 TRIM family

The first definition of the TRIM (tripartite motif-containing proteins) family as a whole dates back to 2001, when Reymond and colleagues identified 37 members in mammals (Reymond et al. 2001). Up-to-date, more than 80 proteins have been classified in humans as part of the TRIM family, based on the similar structure (Hatakeyama 2017). TRIM proteins are represented by a tripartite motif followed by a C-terminal varying domain. The tripartite motif is characterised by three different types of domains and is also referred to as RBCC: a N-terminal RING domain (R), adjacent to either one or two cysteine/histidine-rich motifs known as B-box (B) domain, followed by an alpha-helical coiled-coil (CC) region (Reddy et al. 1992). Most TRIM proteins are considered E3 ubiquitin ligases, due to the presence of a RING domain that recruits E2 enzymes carrying ubiquitin (Giraldo et al. 2020). The B boxes aid in target recognition, while the CC region is necessary for interaction with other TRIM family members and other proteins. Studies have shown that TRIM proteins can form both homo and hetero-interactions through the interplay between CC regions (Meroni & Diez-Roux 2005, Weinert et al. 2015). The C-terminal domain of TRIM proteins is responsible for high specificity in substrate recruitment, as well as for scaffold-function, and may also possess enzymatic activity or RNA binding capacity. Moreover, the C-terminal domain can contribute to epigenetic transcriptional regulation (van Gent et al. 2018).

In addition to their E3 ubiquitin ligase function, TRIM proteins can mediate cellular roles through other mechanisms, such as the elimination of misfolded proteins, which can occur through different pathways, including autophagy and endoplasmic reticulum-associated degradation (Zhang et al. 2020, Saha et al. 2018).

TRIM proteins regulate a wide range of cellular mechanisms, such as cell cycle progression, apoptosis, gene expression, chromatin remodelling, signal transduction, metabolism, neurogenesis, and stem cell biology (Venuto & Merla 2019, Nenasheva & Tarantul 2020). TRIM proteins also play a role in various physiological and pathophysiological processes, such as development, carcinogenesis, and host defence against viral pathogens (Koepke et al. 2021, Petrera & Meroni 2012, Jaworska et al. 2020). Moreover, emerging evidence suggests that TRIM proteins may participate in the modulation of cellular metabolism. Certain TRIM proteins have been implicated in the regulation of energy homeostasis, lipid metabolism, and mitochondrial function (Zhu et al. 2022). TRIM proteins often participate in cellular functions as ubiquitin ligases (Hage & Rajsbaum 2019). However, TRIM proteins have also been implicated in the regulation of transcriptional activity. Some TRIM proteins can directly interact with specific DNA sequences or transcription factors, influencing gene expression patterns. By acting as transcriptional coregulators, TRIM proteins can fine-tune the transcriptional output of specific genes, impacting cellular processes such as development, differentiation, and response to environmental cues. For example, TRIM24, TRIM28 and TRIM33 are transcriptional coregulators that interact with several transcription factors, including the AR. TRIM24 and TRIM28 act together to enhance the AR-mediated transcriptional activity, with TRIM28 being upstream of TRIM24 and protecting it from degradation (Kikuchi et al. 2009, Fong et al. 2018). TRIM33 regulates AR target gene expression by facilitating AR chromatin binding and protecting the AR from degradation (Chen et al. 2022).

1.5.2 TRIM25 in development and disease

The *TRIM25* gene is located on chromosome 17 and is organised in 9 exons. It encodes a 71-kDa protein and is characterised by a RING domain, two B-boxes (B1 and B2) and a PRY-SPRY domain at its C-terminus. The PRY-SPRY domain is involved in recognition of target proteins and RNA binding, and classifies TRIM25 as part of subgroup C-IV (Kwon et al. 2013).
As for other TRIM proteins, TRIM25 has been reported to have a role in several

cellular processes, including innate antiviral immunity, development and maintenance of stemness (Heikel et al. 2016). Finally, it has been reported that TRIM25 contributes to tumour progression. TRIM25 is highly expressed in a variety of cancer types including breast, colorectal, lung, gastric, hepatocellular, urothelial, and endometrial tumours (Sakuma et al. 2005, Qin et al. 2016, Uhlen et al. 2017). Here, TRIM25 plays a significant role in promoting cellular proliferation, migration, and invasion through the regulation of diverse molecular mechanisms. For instance, in lung cancer, TRIM25 is implicated in the ubiquitination of Keap1, a key regulator of the Nrf2 antioxidant pathway, resulting in Nrf2 stabilization and subsequent activation of antioxidant response elements in the promoter of its target genes (Liu et al. 2020). In breast cancer, TRIM25 ubiquitinates 14-3-3 sigma and targets it for degradation, a protein involved in cell cycle arrest and DNA damage response, thereby increasing cell growth and survival (Urano et al. 2002). Additionally, TRIM25 is involved in the regulation of the estrogen receptor in breast cancer, contributing to hormone-dependent tumour progression (Nakajima et al. 2007). Chromatin immunoprecipitation of TRIM25 followed by sequencing in breast cancer cell lines have identified TRIM25 binding sites near genes involved in cell proliferation, migration, and hormone signalling, suggesting that TRIM25 can modulate these processes by controlling the transcription of crucial genes (Walsh et al. 2017). Finally, our lab previously reported that TRIM25 regulated the tumour suppressor p53 by increasing its acetylation in different cell lines, including colorectal cancer cells (Zhang et al. 2015).

1.5.3 TRIM25 in prostate cancer

In PCa, TRIM25 was found to be upregulated in cancerous lesions and, in patients TRIM25 acts as an unfavourable prognostic factor for survival. Consistent with these results, suppressing TRIM25 decreased tumour cell proliferation both in vitro and in vivo (Takayama et al. 2018). In their study, they showed that TRIM25 was necessary for the formation of a complex between the tumour suppressor protein p53 and the GTPase-activating protein-binding protein 2 (G3BP2), which then recruited the SUMO-ligase RanBP2, leading to the SUMOylation of p53 and its translocation from the nucleus. As a result, migration and proliferation

in PCa cells increased as p53-mediated induction of senescence or apoptosis was reduced (Takayama et al. 2018).
Wang et al. found TRIM25 as an ERG (ETS-related gene)-binding partner (Wang et al. 2016). ERG is a transcription factor that promotes the proliferation of PCa cells. The *ERG* gene is frequently fused to the AR-responsive *TMPRSS2* gene. The fusion of these two genes often results in the abnormal expression and activity of ERG, leading to the malignant growth of prostate cells (Tomlins et al. 2005). Interestingly, TRIM25 knockdown upregulated ERG protein levels. TRIM25 was itself found to be a target gene of ERG, thus connecting the two proteins in a negative feedback loop (Wang et al. 2016).
A more recent study, not only confirmed a higher expression of TRIM25 in PCa specimens compared to healthy tissue, but also found a positive correlation between TRIM25 expression and Gleason stages (Li et al. 2022). The authors demonstrated that TRIM25 contributes to tumour malignancy by increasing glucose levels, promoting lipid synthesis and by producing more ATP, needed for a higher cell proliferation rate. Differential expression analysis further revealed that TRIM25 regulated the expression of genes belonging to the tricarboxylic acid cycle, including *IDH1* (isocitrate dehydrogenase 1) and *FH* (fumarate hydratase) (Li et al. 2022).

1.6 Aim of this work

The aim of this project was to investigate the role of TRIM25 in the AR signalling in PCa. PCa is a prevalent malignancy among males, and current therapeutic strategies often involve targeting the AR signalling to suppress tumour growth and progression, yet their long-term efficacy is limited. As a result, there is a growing interest in exploring alternative treatment approaches, such as targeting the coregulators of AR. In this context, understanding the specific role of regulators of AR such as as TRIM25 becomes crucial.
TRIM25 has been implicated in PCa, but its precise contribution to the AR signalling remained to be elucidated. Recent studies conducted by our research group have revealed that TRIM25 controls the stability of p300, a critical coregulator

of the AR. Given that p300 plays a pivotal role in modulating the AR-mediated transcriptional activity, it was particularly interesting to study whether TRIM25 could modulate the AR activity as a transcription factor and how this modulation might occur. The influence of coregulators on AR activity is characterized by their abilities to modify protein abundance, cellular localization, or the binding of AR to the upstream AREs of target genes, amongst others. Thus, these mechanisms were investigated in relation to TRIM25. Moreover, some regulators might modulate AR activity through interplays with each other. For this reason, TRIM25 was studied in the context of p300-dependent effects on AR activity.

By gaining deeper insights into the interactions between TRIM25 and AR, novel mechanisms that could be targeted by therapeutic interventions may be uncovered. This knowledge could potentially lead to the development of more effective treatment strategies for PCa. Exploring the functional impact of TRIM25 on AR activity and its downstream targets holds the potential to identify specific vulnerabilities in PCa cells that can be exploited for therapeutic benefit.

2 Materials and Methods

2.1 Materials

2.1.1 Chemicals

Name	Source
Agarose	Peqlab, Erlangen, Germany
Ammonium Persulfate (APS)	Roth, Karlsruhe, Germany
Bovine Serum Albumine (BSA)	PAA Laboratories GmbH, Pasching, Austria
cOmplete Protease Inhibitor	Sigma Aldrich, Taufkirchen, Germany
Dimethylsuloxide (DMSO)	Fluka, Neu Ulm, Germany
Dithiothreitol (DTT)	Gibco, Invitrogen, Karlsruhe, Germany
DNA Marker 1 Kb	PeqLab, Erlangen, Germany
Dulbecco's Modified Eagle Medium (DMEM)	Gibco, Invitrogen, Karlsruhe, Germany
EDTA	Roth, Karlsruhe, Germany
EGTA	Roth, Karlsruhe, Germany
Ethanol (EtOH)	Roth, Karlsruhe, Germany
Ethidium Bromide	Roth, Karlsruhe, Germany

Continued on next page

Name	Source
FBS (Fetal Bovine Serum)	Gibco, Invitrogen, Karlsruhe, Germany
Acetic Acid	Roth, Karlsruhe, Germany
Glucose	Roth, Karlsruhe, Germany
Glycerol	Roth, Karlsruhe, Germany
Glycine	Roth, Karlsruhe, Germany
GlycoBlue Coprecipitant	Thermo Fisher Scientific, Amsterdam, Netherlands
HEPES	Roth, Karlsruhe, Germany
Hydrogen Chloride	Roth, Karlsruhe, Germany
IGEPAL	Boehringer, Mannheim, Germany
Isopropanol	Roth, Karlsruhe, Germany
Lithium Chloride	Roth, Karlsruhe, Germany
Magnesium Chloride	Roth, Karlsruhe, Germany
Magnesium Sulfate	Roth, Karlsruhe, Germany
Methanol	Roth, Karlsruhe, Germany
N-lauroylsarcosine	Merck, Darmstadt, Germany
Phenol/Chloroform/Isoamyl Alcohol	Thermo Fisher Scientific, Amsterdam, Netherlands
Phosphate Buffered Saline (PBS)	Gibco, Invitrogen, Karlsruhe, Germany
PMSF (phenyl methanesulphonyl fluoride)	Sigma Aldrich, Taufkirchen, Germany
Prestained Protein Ladder	Thermo Fisher Scientific, Erlangen, Germany
Protein Marker	PeqLab, Erlangen, Germany
Roti®-Quant	Roth, Karlsruhe, Germany

Continued on next page

Name	Source
Rotiphorese (Acrylamide/bisacrylamide (30%) (w/v))	Roth, Karlsruhe, Germany
ROX SYBR MasterMix	Eurogentec, Seraing, Belgium
RPMI medium 1640	Gibco, Invitrogen, Karlsruhe, Germany
Sodium Chloride	Roth, Karlsruhe, Germany
Sodium Deoxycholate	Roth, Karlsruhe, Germany
Sodium Dodecyl Sulphate (SDS)	Roth, Karlsruhe, Germany
Tetramethyl ethylen diamine (TEMED)	Roth, Karlsruhe, Germany
Tris-base	Roth, Karlsruhe, Germany
Tris-HCl	Roth, Karlsruhe, Germany
Triton-X-100	Sigma Aldrich, Taufkirchen, Germany
TRIzol	Thermo Fisher Scientific, Erlangen, Germany
Trypsin (0,25%)-EDTA	Gibco, Invitrogen, Karlsruhe, Karlsruhe
Tween 20	Roth, Karlsruhe, Germany
β-mercaptoethanol	Roth, Karlsruhe, Germany

Table 2.1: Chemicals.

2.1.2 Consumables

Name	Source
15-cm cell culture petri dishes	Greiner Bio-One, Nuertingen, Germany

Continued on next page

Name	Source
10-cm cell culture petri dishes	Greiner Bio-One, Nuertingen, Germany
12-well multiwell plates	Greiner Bio-One, Nuertingen, Germany
24-well multiwell plates	Greiner Bio-One, Nuertingen, Germany
96-well PCR Plate	Steinbrenner Laborsysteme GmbH,Wiesenbach, Germany
50 ml reaction tube	Greiner Bio-One, Nuertingen, Germany
15 ml reaction tube	Greiner Bio-One, Nuertingeningen, Germany
2 ml reaction tube	Eppendorf, Hamburg, Germany
1,5 ml reaction tube	Eppendorf, Hamburg, Germany
qPCR sealing film	Steinbrenner Laborsysteme GmbH, Wiesenbach, Germany
20 ml glass pipettes	VWR, Bruchsal, Germany
10 ml glass pipettes	VWR, Bruchsal, Germany
5 ml glass pipettes	VWR, Bruchsal, Germany
1 ml pipetttips	Sarstedt, Nuembrecht, Germany
200 µl pipetttips	Sarstedt, Nümbrecht, Germany
3 ml syringes	Braun, Melsungen, Germany
Sterile filter (pore size 0,22 µm)	Roth, Karlsruhe, Germany
0.2 µl PCR tubes and caps	Sarstedt, Nümbrecht, Germany
Nitrocellulose blotting membrane	Sigma Aldrich, Taufkirchen, Germany
Filter paper	Roth, Karlsruhe, Germany

Table 2.2: Consumables.

2.1.3 Oligonucleotides

All nucleotides were ordered from the company Metabion (Planegg, Germany). They were ordered already dissolved in water at a concentration of 100 µM.

Te following oligonucleotides were used for RT-qPCR:

Name	Sequence (5'-3' direction)
KLK3_F	CCCGGTTGTCTTCCTCACCC
KLK3_R	GCCTCCCCACAATCCGAGACA
TMPRSS2_F	GTCCCCACTGTCTACCAGGT
TMPRSS2_R	CAGACGACGGGGTTGGAAG
c-Myc_F	GCTGCTTAGACGCTGGATTT
c-Myc_R	CTCCTCCTCGTCGCAGTAGA
β-actin_F	CCAACCGCGAGAAGATGA
β-actin_R	CCAGAGGCGTACAGGGATAG

Table 2.3: Oligonucleotides for RT-qPCR.

The following oligonucleotides were used for ChIP-qPCR:

Name	Sequence (5'-3' direction)
KLK3 AREIII_F1	GCCTGGATCTGAGAGAGATA
KLK3 AREIII_R1	ACACCTTTTTTTTTCTGGAT
KLK3 AREIII_F2	GCCCACCTGTTTGTCAGTAA
KLK3 AREIII_R2	ATGAACCTCATGCTGTCTGC
KIAA0066_F	CTAGGAGGGTGGAGGTAGGG
KIAA0066_R	GCCCCAAACAGGAGTAATGA

Table 2.4: Oligonucleotides for ChIP-qPCR.

The following oligonucleotide sequences were used for siRNA silencing:

Name	Sequence (5'-3' direction)
siControl	AACCCCUUUUAAAAGGGGCCCTT
siTRIM25-1	GGGAUGAGUUCGAGUUUCUTT
siTRIM25-2	CUGCGAGGAAUCUCAACAATT

Table 2.5: Oligonucleotides for siRNA silencing.

2.1.4 Lentivirus carrying shRNAs

The lentiviruses carrying short hairpin RNAs (shRNAs) were purchased from Sigma Aldrich. The lentiviral vector used was MISSION pLKO.1-puro, which contains a puromycin resistance gene for efficient selection of transduced cells. A Non-Target-shRNA Control (Product number: SHC016V-1EA) and an shRNA targeting TRIM25 (Clone ID: TRCN0000272649) with a 97% knockdown efficacy were used.

2.1.5 Enzymes

The following enzymes sequences were used for reverse transcription and polymerase chain reaction:

Enzyme	Producer
M-MLV Reverse Transcriptase	Promega
GoTaq G2 DNA polymerase	Promega

Table 2.6: Enzymes for reverse transcription and polymerase chain reaction.

The following enzymes sequences were used for DNA purification after chromatin immunoprecipitation:

Enzyme	Producer
RNase A	Roth
Proteinase K	Merck

Table 2.7: Enzymes for DNA purification.

2.1.6 Plasmids

Plasmid	Description
pcDNA3.1 (+)	Eukaryotic expression vector harbouring a CMV (Cytomegalovirus) promoter for efficient transcription in eukaryotic cells. The plasmid is equipped with a Geneticin (G418) resistance gene, enabling selection in eukaryotes. Additionally, it contains an ampicillin resistance gene for selection in bacteria.
MMTV-luc	Eukaryotic expression vector with a Mouse Mammary Tumor Virus (MMTV) promoter driving the expression of a luciferase reporter gene. Enables convenient monitoring of promoter activity in mammalian cells.
pcDNA3.1-AR-FL	Eukaryotic expression vector, derived from pcDNA.3.1(+), expressing the human full length AR protein. The plasmid was kindly provided by Prof. Andrew Cato.
pcDNA3.1-TRIM25	Eukaryotic expression vector, derived from pcDNA.3.1(+), expressing the human TRIM25 protein.
pcDNA3.1-p300	Eukaryotic expression vector, derived from pcDNA.3.1(+), expressing the human p300 protein.
Renilla luciferase	This reporter construct contains the cDNA of *Renilla reniformis* Luciferase driven by the Ubiquitin promoter.

Table 2.8: Plasmids.

2.1.7 Antibodies

Primary antibodies:

Target	Description	Producer	Application
TRIM25	Mouse monoclonal	BD Biosciences	WB (1:1000) & ChIP
AR (441)	Mouse monoclonal	Santa Cruz Technology	WB (1:1000)
AR (PG-21)	Rabbit	Merck Millipore	ChIP
KLK3 (D6B1)	Rabbit monoclonal	Cell Signaling	WB (1:1000)
p300 (NM11)	Mouse monoclonal	Santa Cruz	WB (1:1000)
β-actin (C-4)	Mouse monoclonal	Santa Cruz Biotechnology	WB (1:1000)
GAPDH	Mouse polyclonal	HyTest	WB (1:50000)
Lamin B (Ab-1)	Mouse monoclonal	Oncogene	WB (1:1000)
PCNA (PC10)	Mouse monoclonal	Santa Cruz Technology	WB (1:1000)
Rabbit IgG	Rabbit polyclonal	Cell Signaling	ChIP

Table 2.9: Primary antibodies.

For Western blotting (WB), primary antibodies were diluted in 5% milk in TBST (20 mM Tris-HCl, 150 mM NaCl, 0.1% Tween-20), with the dilution indicated in the table.
For chromatin immunoprecipitation (ChIP), 5 µg of each antibody was used per sample.

Secondary antibodies:

Target	Description	Producer	Application
Anti-mouse HRP	Goat polyclonal	Dako	WB (1:2000)
Anti-rabbit HRP	Goat polyclonal	Dako	WB (1:2000)

Table 2.10: Secondary antibodies.

Secondary antibodies were conjugated with Horseradish peroxidase (HRP). For Western blotting (WB), they were diluted in 5% non-fat dry milk dissolved in TBST, at a dilution of 1:2000.

2.1.8 Cell lines and cell culture media

Cell line	Source and description
H1299	Human non-small cell lung carcinoma cell line, isolated from the lung of a white, 43-year-old, male patient with carcinoma
LNCaP	Human, androgen-sensitive adenocarcinoma cell line, derived from the left supraclavicular lymph node metastasis of a 50-year old caucasian man diagnosed with metastatic prostate carcinoma (Horoszewicz et al. 1983)
LNCaP NT-1, NT-2	LNCaP cells modified with non-targeting sgRNAs by the CRISPR/Cas9 method. No selection of targeted cells was applied. Cells were kindly provided by Prof. W. Zwart, NKI, Amsterdam
LNCaP KO-1, KO-2	LNCaP cells modified with sgRNAs targeting exon 1 of TRIM25 by the CRISPR/Cas9 method. No selection of targeted cells was applied. Cells were kindly provided by Prof. W. Zwart, NKI, Amsterdam

Table 2.11: Human cancer cell lines.

H1299 cells were cultured in Dulbecco's modified Eagle medium (DMEM) supplemented with 10% fetal bovine serum (FBS) and 1% penicillin/streptomycin.

LNCaP cells, as well as the LNCaP derived cell lines, were cultured in Roswell Park Memorial Institute (RPMI) 1640 supplemented with 10% FBS and 1% penicillin/streptomycin.

2.1.9 Equipment

Measuring devices:

VICTOR Light 1420 Luminsecence Counter, PerkinElmer, Waltham, MA, USA
ChemiDoc™ System, Bio-Rad, Hercules, CA, USA
QuantStudio™ 3 System, Applied Biosystems, Waltham, MA, USA
SpectraMax iD3 System, Molecular Devices, San Jose, CA, USA

Software:

Wallac 1420 Manager, version 3.0, PerkinElmer, Waltham, MA, USA
QuantStudio Design and Analysis Software, version 1.5.1, Fisher Scientific, Waltham, MA, USA
Image Lab Software, version 6.1, Bio-Rad, Hercules, CA, USA
Gene Set Enrichment Analysis (GSEA) software, version 4.1.0, Broad Institute, Cambridge, MA, USA
Adobe Photoshop CS5.1, Adobe Systems Incorporated, San Jose, CA, USA
Microsoft Excel for Mac, version 16.72, Microsoft Corporation, Redmond, WA, USA
R version 4.2.1
RStudio IDE version 2022.12.0+353, RStudio Inc., Boston, MA, USA
TeXstudio version 4.3.1

2.2 Methods

2.2.1 Cell culture and transfection methods

2.2.1.1 Cell culture

All cells were maintained at 37 °C in the incubator with 5% CO_2 and 95% humidity. Cells were confirmed to be mycoplasma-negative and cultured until they reached 80-90% confluence. For subculturing, the medium was aspired. Cells were washed once with sterile phosphate-buffered saline (PBS). 0.25% Trypsin-EDTA was added and cells were incubated at 37 °C until they detached from the culture dish. Culture medium was added in a 1:2 ratio to the cells. The cell-containing solution was transferred into a reaction tube and centrifuged at 1200 rpm for 2 minutes. The supernatant was aspirated and cells were resuspended in fresh culture medium. 25% of the LNCaP cells and 10% of the H1299 cells, respectively, were transferred to a new culture dish containing fresh culture medium.
For long-term storage, cells were removed from the culture dish and collected by centrifugation. Cells were then resuspended in 1 ml of medium supplemented with 20% fetal bovine serum (FBS) and 5% dimethyl sulfoxide (DMSO) and transferred into a cryotube. The cryotube was placed into a cell freezing device that was filled with isopropanol, for slow freezing at -80 °C. For thawing cells, cryotubes were placed at 37 °C in a water bath until the mixture was defrosted. The mixture was transferred to 10 ml of fresh medium and collected by centrifugation. Cells were resuspended in fresh culture medium and transferred to a new culture dish.

2.2.1.2 Counting of cells

Cells were counted using a hemocytometer. First, the hemocytometer was properly washed with ethanol. Then, a clean coverslip was placed over the central square of the hemocytometer.
Cells were detached from the culture dish by trypsinazation. Cells were collected

by centrifugation and diluted in 10 ml culture medium. Using a pipette, 10 µl of cell suspension were added to the gap between the coverslip and the hemocytometer. After that, the hemocytometer was placed under a microscope for cell counting. Starting from the left corner of the counting chamber, cells were systematically counted within the four squares that are at the corners of the grid area. For cells that were at the edges of the grid area, only cells that touched the top and left lines of the squares were counted. At the end, the average number of cells per square was calculated dividing the total number of cells counted by the number of squares (four). To determine the cell concentration in the original cell suspension, the average number of cells per square was multiplied by 10^4, which gave the number of cells per ml.

2.2.1.3 Transfection with calcium phosphate

H1299 cells were trypsinized, resuspended in fresh DMEM medium containing 10% FBS and counted. 6 x 10^5 cells in 4 ml of culture medium were plated per well of a 6-well plate. After plating the cells, 7.42 µg of plasmid DNA were diluted in 180 µl of double distilled water (ddH_2O). 20 µl of a 2.5 M $CaCl_2$ solution were added. 200 µl of a 2X HBS buffer (280 mM NaCl, 1.5 mM Na_2HPO_4, 50 mM HEPES, pH 7.05) were drop-wise added with constantly mixing the sample. The transfection mixture was added to the cell suspension and mixed by gentle swirling. 24 hours later, the medium was aspired and replaced with 2 ml fresh DMEM medium.

2.2.1.4 Transfection with Lipofectamine 3000

Lipofectamine 3000 was used to transfect siRNAs into cells. The day before transfection, 1.3 x 10^4 LNCaP cells were seeded per well of a 24-well plate in 500 µl growth medium. On the day of transfection, the transfection mixes were prepared as follows: for each siRNA, two tubes were prepared; one containing 25 µl growth medium to which 9 µl Lipofectamine 3000 reagent were added. The second tube contained 25 µl growth medium to which 15 pmol siRNA was added.

After gentle vortexing, the two solutions were mixed together, vortexed again and incubated for 15 minutes at room temperature. After incubation, the mixture was drop-wise added to the cells. After 20 hours the medium was removed and fresh medium was added to the cells. Cells were incubated for further 24 hours.

2.2.1.5 Infection of cells with lentivirus

Infection was performed according to Sigma-Aldrich MISSION® instructions. The day before infection, 1.6 x 10^4 cells were seeded per well of a 96-well plate. On the day of infection, the culture medium was replaced with 110 µl of fresh medium. Lentiviral particles were added to the cells at the multiplicity of infection (MOI) of 5. Cells were incubated for 24 hours, after which the medium was replaced with 120 µl fresh culture medium. 48 hours later, the medium was removed and replaced with fresh medium containing 1 µg/ml puromycin. Control cells that had not been infected with lentivirus were also treated with puromycin to determine the time needed to eliminate non-resistant cells. Medium was replaced every 3-4 days with fresh puromycin-containing medium. Resistant cells were expanded.

2.2.1.6 Dual reporter assay

For the analysis of androgen receptor activity, 6 x 10^5 H1299 cells in phenol red-free DMEM medium supplemented with 3% charcoal-stripped FBS (CSS) were plated per well of a 6-well plate. Cells were transfected with 0.12 µg Renilla, 1.8 µg MMTV-luciferase, 0.5 AR µg, 2.5 µg TRIM25, 2.5 µg p300 plasmids. 24 hours after transfection, the medium was replaced with fresh phenol red-free DMEM medium with 3% CSS and 10 nM DHT or ethanol were added. 24 hours after treatment, cells were washed with ice-cold PBS and lysed with 1X Passive Lysis Buffer (Promega, Mannheim, Germany) for 20 minutes on ice.
To determine the firefly-luciferase activity, 20 µl of the lysate were trasferred into a 96-well luminometer plate and the plate was placed into a Victor Light 1420 Luminescence Counter. 70 µl of Gly-Gly-Buffer (25 mM Glyglycin, 15

mM $MgSO_4$, 1 mM DTT and 0.1 mM ATP) and 20 µl of luciferin solution (1 mM firefly luciferin, 25 mM Glyglycin, 15 mM $MgSO_4$, 4 mM EGTA) were autoinjected per well and the luciferase activity was measured by the device.
For the measurement of renilla luciferase activity, 20 µl of the lysate were trasferred into a 96-well luminometer plate and the plate was placed into a Victor Light 1420 Luminescence Counter. 100 µl of Coelenterazin-Buffer (0.1 M potassium phosphate buffer, 0.5 M NaCl, 1 mM EDTA, pH 7.6, 0.2 nM Coelenterazin) were autoinjected and luciferaserase activity was measured by the device.
The relative luciferase activity was calculated by dividing the firefly luciferase activity by the renilla luciferase activity.

2.2.1.7 MTT assay

3 x 10^3 cells were seeded per well of a 96-well plate. A total of 200 µl growth medium was used for each well. After incubation of the cells for the desired time, MTT (3-(4,5-dimethylthiazol-2-yl)-2,5-diphenyltetrazolium bromide) solubilized in PBS was added to each well at a final concentration of 0.5 µg/µl. After an incubation time of 2 hours, the medium was removed without disturbing the formazan crystals at the bottom of the wells. 200 µl isopropanol were added and the crystals were dissolved by gentle shaking. The absorbance of the isopropanol-formazan solution was measured at 590 nm, using a microplate reader.

2.2.2 Protein methods

2.2.2.1 Preparation of cell lysate

Cells were washed twice with ice-cold PBS, collected with a rubber cell scraper and transferred to reaction tubes. Cells were collected by centrifugation and the residual PBS was removed. The cell pellet was lysed in NP-40 buffer (150 mM NaCl, 50 mM Tris pH 8.0, 5 mM EDTA, 1% IGEPAL, 1 mM PMSF). The lysate was kept on ice for 10 minutes to allow proper disruption of cells, followed by

centrifugation at 13000 rpm at 4 °C for 10 minutes. The supernatant was retained and protein concentration was determined.

2.2.2.2 Cell fractionation

After aspirating the medium, cells were washed twice with ice-cold PBS, scraped from the plate and transferred to a microcentrifuge tube. Cells were collected by centrifugation and resuspended in an equal volume of ice-cold fractionation buffer (10 nM HEPES pH 7.5, 10 mM KCl, 1 mM EGTA, 1 mM EDTA, 1 mM DTT, 1 mM PMSF) and kept on ice for 15 minutes. IGEPAL was added to a final concentration of 6% in fractionation buffer and the sample was vortexed, followed by centrifugation at 13000 rpm at 4 °C for 15 minutes. The supernatant, which contained the cytoplasmic fraction, was transferred to a new tube. The pellet was washed three times with 500 µl fractionation buffer to remove any cytoplasmic contamination. The pellet was resuspended in 1/3 volume of nuclear buffer (20 mM HEPES pH 7.9, 400 mM NaCl, 1 mM EDTA, 1 mM EGTA, 1 mM DTT, 1 mM PMSF) of the fractionation buffer used at the beginning to lyse the cells. This lysate, which contained the nuclear fraction, was sonified for 15 minutes with 30 seconds-intervals (30" on, 30" off) at 4 °C. Thereafter, the sample was incubated on ice for 20 minutes and vigorously vortexed every 5 minutes to facilitate the solubilization of nuclear proteins. Finally, both cytoplasmic and nuclear fractions were cleared by centrifugation at 13000 rpm at 4 °C for 5 minutes. The supernatant was transferred into a new tube and the protein concentration was determined. 45 µg of sample were diluted in 2X SDS buffer, heated to 95 °C for 5 minutes, loaded onto an SDS-PAGE gel and blotted onto a nitrocellulose membrane. Detection of GAPDH and Lamin B was used to visualize the cytoplasmic and nuclear fraction, respectively.

2.2.2.3 Determination of protein concentration

The Bradford working solution was prepared by diluting a 5X concentrated stock (Roti®-Quant) in water. To determine the protein concentration of each sample, 2

µl of the sample were added to 500 µl of Bradford working solution and measured at 595 nm. For the calibration curve, 2 µl of lysis buffer were added to the Bradford solution. On top of that, 0, 2, 4 or 6 µl of a BSA (bovine serum albumin) solution (1 mg/ml) were added to 500 µl Bradford reagent and measured in parallel. The protein sample concentration was determined by fitting a curve to the optical density (OD) values of different volumes of BSA. From this curve, the OD value corresponding to 1 µl of BSA was obtained and named α. The OD of the sample was used to find its concentration, with the formula OD/2α. Typically, 45 µg of protein extract were resolved by SDS-polyacrylamide gel electrophoresis.

2.2.2.4 SDS-polyacrylamide gel electrophoresis

The sodium dodecyl sulfate polyacrylamide gel electrophoresis (SDS-PAGE) was prepared by utilizing the Bio-Rad casting system to cast the gels and conduct the electrophoresis. 8 or 10% gels were employed for every experiment. Plastic casting stands and frames were used to hold a pair of glass plates with a space of 1.5 mm in between. First, 20 ml of resolving gel were prepared as follows:

Ingredient	**8% gel**	**10% gel**
Acrylamide mix	5.3 ml	6.7 ml
H_2O	9.3	7.9 ml
Tris 1.5 M pH 8.8	5 ml	5 ml
SDS	0.2 ml	0.2 ml
APS	0.2 ml	0.2 ml
TEMED	0.012 ml	0.008 ml

Table 2.12: Resolving gel recipe.

The gel was poured into the space between the glass plates, up to 2 cm below the top of the smaller glass plate. Isopropanol was used to overlay the gel. After polymerization, the isopropanol was washed away with distilled water and 5 ml of stacking gel were prepared as follows:

Ingredient	Volume
Acrylamide mix	0.83 ml
H_2O	3.4
Tris 1.5 M pH6.8	0.63 ml
SDS	0.05 ml
APS	0.05 ml
TEMED	0.005 ml

Table 2.13: Stacking gel recipe.

The stacking gel was poured onto the resolving gel. A comb with an appropriate number of wells was inserted into the stacking gel. When the stacking gel was polymerized, the comb was removed, the glass plates with the gel were fixed in the electrophoresis chamber, and the chamber was filled with running buffer (25 mM Tris, 200 mM glycin, 0.1% SDS). Samples were mixed with an equal volume of SDS sample buffer (4% sodium dodecyl sulfate, 0.16 M Tris pH 6.8, 20% glycerol, 4% β-mercaptoethanol, 0.002% bromophenol blue) and heated to 95 °C for 5 minutes to denature the proteins. After loading of the samples onto the SDS gel, samples were run at 100 V until they passed the stacking gel and then at 120 V until the bromophenole blue front reached the end of the gel.

2.2.2.5 Western blotting

The proteins that were separated by SDS-PAGE were transferred onto a nitrocellulose membrane. The membrane was first wetted with distilled water. A sandwich of sponge/three filter papers/gel/membrane/three filter papers/sponge was prepared in a cassette immersed in transfer buffer (25 mM Tris, 200 mM glycin, 10% methanol, in H_2O). When the sandwich was ready, the cassette was clamped tightly and excluding air bubbles. The cassette was positioned in a transfer chamber and the chamber was filled with transfer buffer. The transfer system was placed into an ice-bucket and fully covered by ice. The proteins were transferred at 100 V for 2 hours.

2.2.2.6 Immunodetection

After the transfer, the membrane was incubated in blocking solution (5% milk powder dissolved in TBST) for 45 minutes at room temperature with gentle shaking. To detect the proteins of interest, the membrane was incubated with primary antibodies diluted in blocking solution overnight at 4 °C with constant shaking. The day after, the membrane was washed three times with TBST for 5 minutes each. After that, the membrane was incubated with a HRP-conjugated secondary antibody diluted in blocking solution for 1.5 hours at room temperature with constant shaking. The membrane was then washed as previously and the detection of the proteins was achieved using equal volumes of enhancer of chemioluminescence (ECL) reagent I (100 mM Tris-HCl, pH 8.5, 2.5 mM luminol, 400 µM coumaric acid) and ECL reagent II (100 mM Tris-HCl, pH 8.5, 0.02% H_2O_2). Chemiluminescent signals were detected with a ChemiDoc detection device.

2.2.2.7 Mass spectrometry

3 x 10^6 cells were seeded and cultured for 48 hours until they reached 70-80% confluence. The medium was aspired and cells were washed twice with ice/cold PBS. Cells were harvested in ice-cold PBS with a plastic scraper and collected by centrifugation. The cell pellet was quickly frozen in liquid nitrogen and stored at -80 °C until it was sent to the Proteomics/Mass Spectrometry facility at the NKI in Amsterdam, for protein determination and analysis of the data. The data were provided as tables containing $\log_2$-transformed label-free quantitation (LFQ) intensities by the Proteomics/Mass Spectrometry facility for further analysis.
The data tables were imported into R. Using these values, fold changes were calculated and p-values were determined using Student's t test. The obtained results were visualized using volcano plots that were generated with the EnhancedVolcano package (Blighe et al. 2019). These plots depict the $\log_2$ fold change on the x-axis and the $\log_{10}$-transformed p-value on the y-axis. Specific cutoffs were chosen to highlight proteins with significant differential expression. A fold change threshold of 1.5 was used to identify genes that exhibited a minimum absolute fold change of 1.5 between the conditions being compared. In addition, a p-value

threshold of 0.05 was applied to identify genes with statistically significant differential expression. Genes with p-values below this threshold were considered to have a significant level of differential expression, indicating that the observed expression differences were unlikely to occur by chance.
With fold change values, Gene Set Enrichment Analysis (GSEA) was performed on the GSEA software developed by the Broad Institute (Subramanian et al. 2005). To perform the analysis, a CSV file containing all proteins included in the study was created, with data ranked based on their $\log_2$ fold change values in decreasing order, and converted into an rnk file format. The rnk file was then imported into the GSEA software, and the "pre-ranked" tool was utilized to execute the analysis on the Hallmark signature.

2.2.3 RNA analysis

2.2.3.1 RNA extraction

Cells were washed twice with ice-cold PBS, collected with a rubber cell scraper and transferred to a microcentrifuge tube. Cells were collected by centrifugation with a bench top centrifuge for 10 seconds and the residual PBS was removed. The cell pellet was resuspended and lysed in TRIzol. To allow for complete dissociation of nucleoprotein complexes, the tube was then incubated at room temperature for 5 minutes. 1/5 volume of chloroform was then added and the tube was vigorously shaked until the sample was properly homogenized. The sample was then incubated at room temperature for 10 minutes and consequently centrifuged at 13000 rpm at 4 °C for 10 minutes to allow for phase separation. The upper aqueous phase, containing RNA, was carefully transferred to a new RNase-free microcentrifuge tube. 1/2 volume of isopropanol of the initial amount of TRIzol was added and the sample was incubated on ice for 10 minutes, or at -20 °C overnight. After centrifugation at 13000 rpm at 4°C for 10 minutes, the supernatant was removed and the RNA pellet was washed twice with 75% ethanol. After the second wash, the ethanol was removed carefully and the RNA pellet was air-dried for 5-10 minutes. Finally, the RNA pellet was dissolved in 30 µl RNA-free water and the RNA concentration was determined using a NanoDrop.

2.2.3.2 Complementary DNA (cDNA) synthesis

1 µg of RNA was incubated with 0.5 µl of ribonuclease and 1 µl of DNase in 1X DNase buffer in a total reaction volume of 20 µl, at 37 °C for 1 hour. 2 µl of DNase Stop Solution were added and incubated at 65 °C for 10 minutes to inactivate the DNase. The sample was mixed with 2 µl random primers (200 ng/µl) and heated to 70 °C for 5 minutes to allow the primers to anneal to the RNA. After primer annealing, the sample was divided into two tubes. 1 µl reverse transcriptase M-MLV RT, 0.125 µl dNTPs (10 mM) and 4 µl 5X M-MLV RT buffer were added to one tube, whilst the same mix without M-MLV RT was added to the second tube as negative control. The reaction was incubated in a thermocycler as follows:

Step	Temperature	Time
1	25 °C	10 min
2	42 °C	60 min
3	70 °C	10 min
4	4 °C	Infinite

Table 2.14: Program for first strand cDNA synthesis.

After cDNA synthesis, each product was diluted with 100 µl RNase-free water and a control PCR was performed.

2.2.3.3 Quality control polymerase chain reaction (PCR)

A quality control PCR was performed to see whether reverse transcription was successful and without any genomic DNA contaminants.
4 µl of cDNA were mixed with 0.125 µl GoTaq Polymerase, 0.125 µl dNTPs (10 mM), 1 µl forward and 1 µl reverse primers (10 µM) for actin, 4 µl 5X GoTaq Polymerase Buffer and adjusted to a final volume of 20 µl with ddH_2O. The reaction was run in a thermocycler with the following conditions:

Step	Temperature	Time	Cycle
1	95 °C	1 min	1X
2	95 °C	20 sec	40X
	65 °C	20 sec	
	72 °C	30 sec	
3	4 °C	infinite	1X

Table 2.15: Quality control PCR settings.

In the meanwhile, agarose powder was mixed with 1X TAE buffer (40 mM Tris, pH 7.2, 20 mM sodium acetate, 1 mM EDTA) to a final concentration of 2%. The mixture was heated in a microwave with intermittent swirling, until the agarose was completely dissolved. The solution was then cooled and ethidium bromide was added to a final concentration of 0.3 µg/ml. The solution was poured on a gel tray and let solidify. The PCR products were finally run on the 2% agarose gel and visualized under UV light.

2.2.3.4 Quantitative Real Time PCR (RT-qPCR)

For each target gene, a mix containing 10 µl SYBR Green reagent, 1 µl forward primer (10 µM), 1 µl reverse primer (10 µM) and 4 µl water was prepared per well of a 96-well qPCR plate. 4 µl of cDNA were also added to the well. After brief centrifugation of the plate, the RT-qPCR was performed with the following settings:

Step	Temperature	Time	Cycle
Denaturation	95 °C	10 min	1X
Amplification	95 °C	15 sec	40X
	60 °C	60 sec	
Melting curve	95 °C	15 sec	1X
	60 °C	60 sec	
	95 °C	15 sec	

Table 2.16: qPCR settings.

The mRNA expression of a target gene was calculated from the Ct value given by the qPCR machine for this gene, relatively to the Ct value of a reference gene, according to the $\Delta\Delta$Ct method.
First, the ΔCt of a control group and of an experimental sample was calculated as follows:

$$\Delta\text{Ct} = \text{Ct(gene of interest)} - \text{Ct(reference gene)}$$

Afterwards, the $\Delta\Delta$Ct was obtained as the difference between the ΔCt of the experimental group and that of the control group:

$$\Delta\Delta\text{Ct} = \Delta\text{Ct(experimental group)} - \Delta\text{Ct(control group)}$$

Finally, the fold change in gene expression was calculated as:

$$\text{Fold Change} = 2^{-\Delta\Delta\text{Ct}}$$

2.2.3.5 RNA-sequencing

For transcriptomic analysis, 6 x 10^5 cells were seeded and harvested in ice-cold PBS 48 hours after seeding. Cell pellets were stored at -80 °C and submitted to the NKI Genomics Core facility in Amsterdam, for RNA extraction, library

preparation and sequencing. The facility also performed the data analysis, including annotation, alignment and counting of the reads. The reference genome used for alignment was hg38, and the RNA-seq data were generated using pair-end sequencing.

The read count matrix was imported into R, where the DESeq2 package (Love et al. 2014) was installed and loaded for subsequent analysis. The raw gene-level count data obtained from the RNA-seq analysis were converted into counts per million (CPM) values. To calculate CPM values, the raw counts data was normalized by dividing each count by the respective library size (total counts) for the corresponding sample and scaling by a factor of one million. This normalization approach enabled a fair comparison of gene expression levels across samples. The CPM values were particularly useful for analyzing and comparing the expression levels of the target gene (TRIM25) between the control and knockout samples. To visualize the CPMs for TRIM25 in each sample into a plot, the ggplot package (Wickham 2016) in R was utilized.

For principal component analysis (PCA) the count data was normalized using DESeq2's normalization method. The variance stabilizing transformation (VST) adjusted the counts for each gene across samples. The VST-transformed data was used as input for the PCA analysis. The resulting PCA plot provided a visual representation of the similarities and dissimilarities between samples based on their gene expression profiles.

For differential analysis, two approaches were taken: DESeq2 (Love et al. 2014) and limma (Ritchie et al. 2015). With DESeq2, the count matrix containing the read counts was prepared and formatted as a DESeqDataSet object. Normalization of the count data was then carried out using the DESeq2 algorithm, which modelled the dispersion of gene expression, taking into account both biological and technical variability. This way, DESeq function calculated the dispersion parameters and performed statistical tests to identify genes with significant differential expression between the experimental conditions. The obtained p-values were again adjusted using the Benjamini-Hochberg procedure. Gene annotations were retrieved using the Ensembl IDs and the org.Hs.eg.db package (Carlson et al. 2019). After performing the differential expression analysis using DESeq2, the results were further visualized using volcano plots. The volcano plots provide

a concise representation of the fold change and statistical significance of gene expression differences between different conditions. To create the volcano plots, the EnhancedVolcano package was employed (Blighe et al. 2019). For the volcano plots, specific cutoffs were chosen to highlight genes with significant differential expression. The fold change threshold of 1.3 was used to identify genes that exhibited a minimum absolute fold change of 1.3 between the conditions being compared. In addition, a p-value threshold of 0.05 was applied to identify genes with statistically significant differential expression. Genes with p-values below this threshold were considered to have a significant level of differential expression, indicating that the observed expression differences were unlikely to occur by chance.

For differential expression analysis with limma, a DGEList object was created, combining the count data and the sample metadata. Low-expressed genes were filtered out based on expression levels, with a log-fold-change cutoff of 0. This ensured that only genes with significant changes in expression across the specified groups were retained for further analysis. The count data was normalized using the TMM (trimmed mean of M-values) method. A design matrix was constructed to represent the experimental conditions, comparing the groups of interest. By fitting this model, voom function estimated coefficients for each gene, representing the differences in gene expression between the experimental groups. Empirical Bayes moderation was applied to the estimated coefficients, which shrunk the fold changes towards a common value, improving the accuracy of the estimates, particularly for genes with low counts or high variability. Gene annotations were retrieved using the Ensembl IDs and the org.Hs.eg.db package (Carlson et al. 2019). After obtaining the differential expression results using limma, the output was further utilized for GSEA on the Hallmark gene sets using the clusterProfiler package (Wu et al. 2021). GSEA function used a list of fold changes as input, and parameters such as minimum (3) and maximum (800) gene set sizes and the Benjamini-Hochberg method for p-value adjustment were specified. The statistically significant Hallmark pathways were visualized using barplots generated with the ggplot package.

Further analysis focused on genes associated with the Hallmark Androgen Response. The gene list corresponding to this geneset was obtained and used

to select genes of interest for further analysis. To perform normalization, the variance-stabilized data (vsd) obtained from the DESeq2 analysis was utilized. Row means of vsd were obtained and subtracted from the vsd data to achieve normalization. Subsequently, the normalized data was subjected to gene filtering and visualized using a heatmap generated with the pheatmap package (Kolde 2019). The colours in the heatmap indicate the relative expression levels of genes in different samples.

2.2.4 Chromatin immunoprecipitation (ChIP)

Using a total of five cell culture dishes, 5 x 10^6 cells were seeded per dish onto 15-cm culture plates. The cells were cultured until reaching 70-80% confluence. The day before cell lysis, 50 µl protein G dynabeads or protein A agarose beads were washed 3 times with 0.5% BSA in PBS. After the last wash, 50 µl BSA/PBS and 5 µg of antibody were added to the beads. The antibody-beads mixture was placed on a rotor to allow for coupling overnight.
Formaldehyde was added directly to the cell culture medium to a final concentration of 1% and incubated for 10 min at room temperature with gently shaking of the dishes to enable crosslinking of protein-DNA complexes. To quench the crosslinking reaction, glycine was added directly to the cell culture medium to a final concentration of 125 mM. The cells were incubated for an additional 5 minutes to ensure complete quenching of formaldehyde. The cells were then washed twice with ice-cold PBS and scraped from the dish in PBS supplemented with 1X protease inhibitor cocktail. The cells were collected by centrifugation at 2000 rpm for 5 minutes at 4 °C and stored at -80 °C.
The cell pellet was resuspended in 15 ml lysis buffer 1 (50 mM HEPES, 140 mM NaCl, mM EDTA pH 8, 10% glycerol, 0.5% IGEPAL, 0.25% Triton X-100) containing 1X protease inhibitor cocktail. The cell suspension was incubated on a rotor at 4 °C for 10 minutes to allow for cell lysis. After centrifugation at 2000 rpm for 5 minutes, the supernatant was removed and the cell pellet was resuspended in 15 ml lysis buffer 2 (10 mM Tris, 200 mM NaCl, 1 mM EDTA, 0.5 mM EGTA) and the same procedure was repeated. The cell pellet was again resuspended in 1.5 ml lysis buffer 3 (10 mM Tris, 100 mM NaCl, 1 mM EDTA, 0.5 mM EGTA,

0.1% Na-deoxycholate, 0.5 % N-lauroylsarcosine).
The cell suspension was divided into 5 microcentrifuge tubes and the chromatin was sheared by sonication for 10 cycles (30" on, 30" off) to obtain DNA fragments of sizes ranging from 200 to 500 bp. After sonication, the volumes of the 5 tubes were pooled into one tube, and 1% Triton-X was added. The sample was centrifugated at 14000 rpm at 4 °C for 12 minutes to remove cellular debris. The supernatant was collected into a fresh tube and 50 µl were separated into a new tube and stored as input. 50 µl of the pre-coupled and washed beads were added to the supernatant and the mixture was incubated overnight at 4°C with gentle rotation. The day after, the immunoprecipitated chromatin complexes were washed 10 times with RIPA buffer (50 mM HEPES, 500 mM LiCl, 1 mM EDTA, 1 % IGEPAL, 0.7% Na-DOC) and 1 time with TBS buffer (20 mM Tris, 150 mM NaCl). Both input and immunoprecipitates were diluted with 200 µl elution buffer (50 mM Tris, 10 mM EDTA, 1 % SDS) and the tubes were heated to 65 °C for 18 hours to reverse crosslinks. After decrosslinking, the beads were discarded and the eluted DNA was mixed with 200 µl TE buffer (10 mM Tris, 1 mM EDTA), treated with 0.9 µl RNse A (10 mg/ml) and incubated at 37 °C for 1 hour to remove RNA contaminants. The sample and input were subsequently treated with 4 µl proteinase K (20 mg/ml) and incubated at 55 °C for 2 hours to digest proteins. After that, the DNA was extracted with 400 µl phenol/chloroform/isoamyl alcohol mixture (ratio 25:24:1), followed by centrifugation at 10000 rpm for 5 minutes. The upper part was transferred to a new microcentrifuge tube and 15 µl NaCl (5 M) and 1.5 µl Glycoblue were added, as well as 800 µl ice-cold ethanol. The mixture was vortexed and incubated for 1 hour at -80 °C to allow precipitation of the DNA fragments. After centrifugation at 14000 rpm at 4 °C for 30 minutes, the supernatant was removed and the DNA pellet was washed with ethanol 80%. At the end, the DNA pellet was air-dried at 50 °C and then diluted in 50 µl 10 mM Tris-HCl pH 8.0.

2.2.4.1 ChIP-sequencing

Samples were sent to the Genomics Core facility at the NKI in Amsterdam, for library preparation and sequencing. The facility was also responsible for analysis

of the data, including peak calling. BigWig files were provided for further analysis and visualization.
The visualization of ChIP-seq data was performed using the Integrative Genomics Viewer (IGV, Robinson et al. (2011)), a widely used software for the interactive exploration of genomic data. BigWig files containing signal intensity information were loaded into IGV to generate visual representations of the ChIP-seq data.

2.2.4.2 ChIP-qPCR

For qPCR, the same protocol was used as described in Section 2.2.3.4. To analyse the data, the Ct value of the ChIP sample was first normalized by the Ct value of the input as follows:

$$\text{Normalized Ct} = \text{Ct(ChIP sample)} - \text{Ct(Input)}$$

After that, the ΔCt was calculated by subtracting the normalized Ct of a reference sequence to the normalized Ct of a target sequence:

$$\Delta\text{Ct} = \text{Normalized Ct(target sequence)} - \text{Ct(reference sequence)}$$

The $\Delta\Delta$Ct was obtained for experimental sample over control sample:

$$\Delta\Delta\text{Ct} = \Delta\text{Ct(experimental group)} - \Delta\text{Ct(control group)}$$

Finally, the fold change was calculated as:

$$\text{Fold Change} = 2^{-\Delta\Delta\text{Ct}}$$

An IgG control was included to validate and confirm that any observed modulation of the protein-DNA interactions between the experimental conditions was specific to the protein of interest.

2.2.5 Statistical analyses

The experiments conducted in this study included a minimum of three replicates. To assess differences between two groups, statistical analysis was performed using Student's t-test. For multiple comparisons, one-way ANOVA followed by Tukey's test was employed. In cases where two factors were investigated, such as treatment and knockout, data were analyzed using two-way ANOVA followed by Tukey's test. The data was expressed as means ± standard deviation, and statistical significance was determined at a p-value smaller than 0.05. All statistical analyses were performed using Microsoft Excel 2019 and R 2022.

3 Results

3.1 Effects of TRIM25 on the AR signalling

3.1.1 TRIM25 reduces AR activity

Our laboratory previously found that TRIM25 reduced the activity of AR in a dual reporter assay (Pauletto et al. in revision). To confirm these findings, the H1299 cells were transfected with plasmids encoding AR, TRIM25, a reporter where the MMTV promoter was fused to the firefly luciferase gene, and renilla luciferase, with the latter used as a normalization control. The cells were seeded in phenol red-free DMEM culture medium, supplemented with 3 % charcoal-stripped FBS (CSS) and incubated for 48 hours to starve the cells. The cells were then treated with either 10 nM DHT for 24 hours or with the vehicle ethanol. The cells were harvested and lysed, and a dual reporter assay was performed.
Significantly reduced levels of AR activity were observed when TRIM25 was overexpressed (Figure 3.1). These findings confirm that TRIM25 plays a role in regulating the AR activity, and suggest that it may act as a negative regulator of the AR-mediated transcriptional activity.

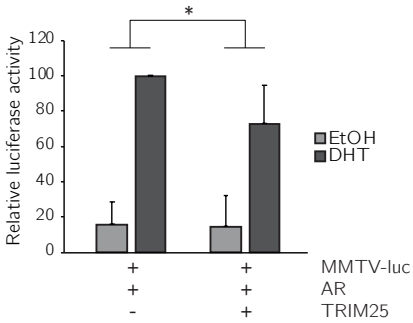

Figure 3.1: TRIM25 decreased the activity of AR. H1299 cells were transfected with plasmids encoding AR, TRIM25, MMTV-firefly luciferase and renilla luciferase (for internal control). After starvation for 48 hours, cells were treated with 10 nM DHT or ethanol for 24 hours and dual reporter assays were performed. The luminescence values of the firefly luciferase were normalized by the renilla luciferase luminescence values. The luciferase activity when AR was overexpressed and cells were treated with DHT was set to 100. The graph represents mean values and standard deviations of 5 independent experiments. The p-value was calculated using two-way ANOVA followed by Tukey's test. * = p-value < 0.05

3.1.2 TRIM25 influences AR target gene profile

In order to expand the investigation of the regulatory impact of TRIM25 on AR regulated genes, its influence on the entire transcriptome was studied. To do that, LNCaP cells were subjected to CRISPR/Cas9-mediated knockout of the *TRIM25* gene using two distinct guide RNAs, resulting in the generation of the TRIM25-knockout cell lines KO-1 and KO-2. Two non-targeting guide RNAs were utilized as controls, leading to cell lines NT-1 and NT-2. RNA-sequencing was performed on these cell lines and the transcript levels of TRIM25 were detected for all samples and plotted as per Appendix Figure A.1A. This figure shows a clear reduction of TRIM25 in the KO cell lines with TRIM25 expression being even lower in the KO-2 cells compared to the KO-1 cells (Figure A.1A). To check TRIM25 protein levels in these cell lines, NT-1, NT-2, KO-1 and KO-2 cells were collected and lysed for Western blotting. Appendix Figure A.1B shows decreased levels of TRIM25 protein in the KO-1 and KO-2 cell lines compared to the controls NT-1 and NT-2 (Figure A.1B).

After conducting the differential analysis on the RNA-sequencing counts, Principal Component Analysis (PCA) was performed to gain insight into the overall variability and relationships between samples. As shown in Appendix Figure A.1C, the two non-targeted cell lines clustered closely together, exhibiting a minimal variance (19%). Likewise, the two knockout cell lines clustered closely together, while there was a clear difference between the clusters of KO cells and NT control cells (Figure A.1C).
Differential analysis using the DESeq2 R package enabled the determination of fold changes and p-values for all genes. The comparisons were carried out by contrasting each knockout cell line (KO-1 and KO-2) with the combined non-targeted control group (NTs, comprising NT-1 and NT-2). To visualize the results, volcano plots were generated.

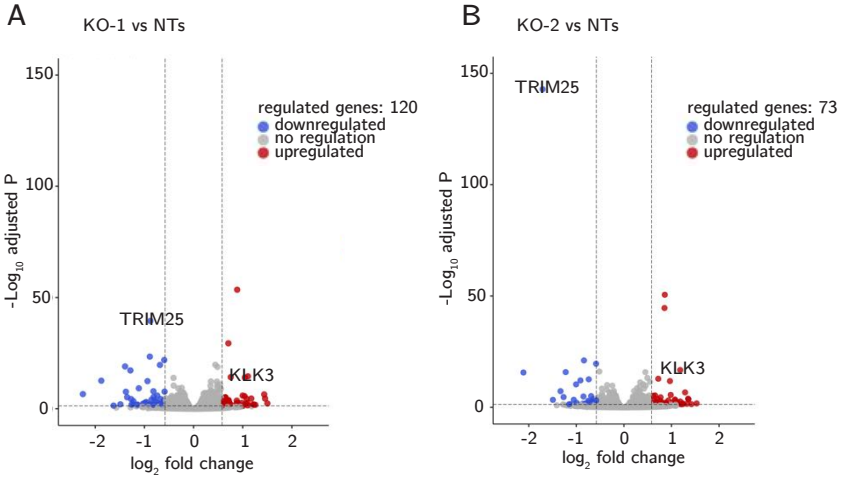

Figure 3.2: TRIM25 influences gene transcription. LNCaP cells were subjected to RNA-sequencing after CRISPR/Cas9-mediated knockout of TRIM25 (KO-1 and KO-2). As controls, two non-targeted cell lines were included, and their samples were pooled together (NTs). The experiment was conducted in triplicates. Volcano plots were generated to show differences in the gene expression profile of KO-1 vs NTs (**A**) and KO-2 vs NTs (**B**). The x-axis represents the $\log_2$ fold change, and the y-axis represents the -Log_{10} adjusted P value. Genes with a fold change greater than 1.3 (absolute value) and an adjusted p-value of less than 0.05 were considered significantly regulated. Blue dots indicate genes that are significantly downregulated and red dots indicate genes that are significantly upregulated.

It was found that KO-1 regulated a total of 120 genes, while KO-2 regulated 73 genes. One of the highly regulated genes was *KLK3*, a well-known AR target gene, indicating a potential increase in AR activity due to TRIM25 knockout (Figure 3.2).

To check if TRIM25 could increase the AR response in the LNCaP cells, the list of fold changes for each gene was used to perform Gene Set Enrichment Analysis (GSEA) on the Hallmark gene sets.

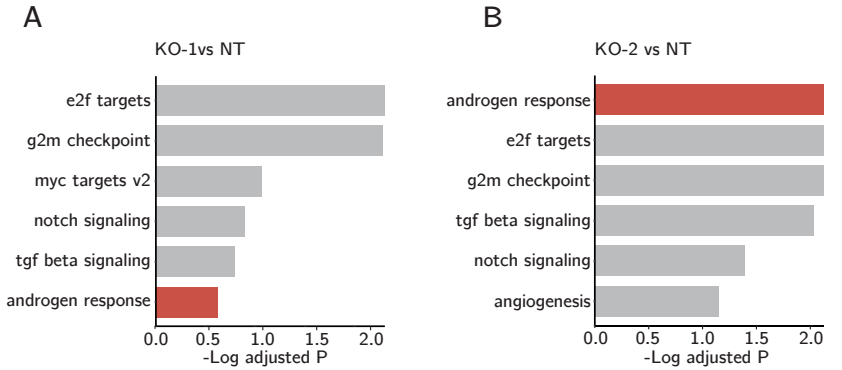

Figure 3.3: TRIM25 knockout induces the androgen response. Gene Set Enrichment Analysis (GSEA) was performed on the Hallmark signature to visualize the regulated gene sets. Bar graphs show the enriched datasets for KO-1 vs NT (**A**) and KO-2 vs NT (**B**). The y-axis shows the -$\log_{10}$ adjusted p-value, indicating the significance of enrichment.

GSEA revealed that the Hallmark Androgen Response pathway was activated by both knockouts, although the adjusted p-value for KO-1 was just below the false discovery rate (FDR) threshold of 0.05 (adjusted P = 0.058) (Figure 3.3).

Next, the genes belonging to the Hallmark Androgen Response pathway were examined to visualize changes in expression levels across different samples. Figure 3.4 displays the normalized expression values for the genes that exhibited significant changes in gene expression in the knockouts compared to the NT controls. The stronger upregulation (in red) included the canonical AR target genes *KLK3* and *TMPRSS2* (Figure 3.4).

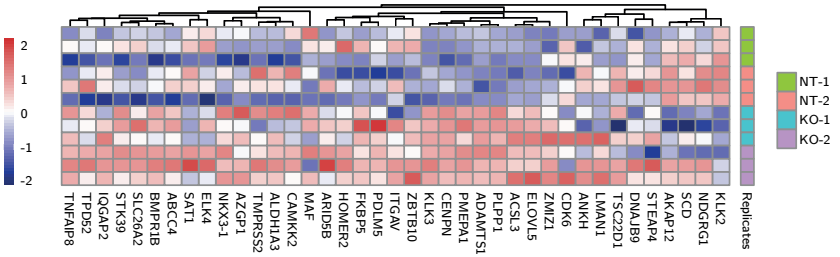

Figure 3.4: Hallmark Androgen Response genes that are regulated by TRIM25. Heatmap displaying the vsd (variance-stabilized data) values normalized by calculating the row-wise mean of the vsd values for genes in the Hallmark Androgen Response dataset that showed regulation upon TRIM25 knockout. The columns represent individual genes, while the rows represent different samples and replicates. The colour intensity represents the expression level of each gene, with higher values indicated by darker shades.

These results confirm the initial results that TRIM25 controls AR activity, with KO-2 showing a stronger impact on the Hallmark Androgen Response pathway. The upregulation of canonical AR target genes in the knockout cells further supports a potential modulation of AR activity resulting from the knockout of TRIM25.

To validate the findings obtained from RNA-seq, RT-qPCR was performed for the expression of *KLK3* and *TMPRSS2*. The RT-qPCR results showed significant upregulation of *KLK3* and *TMPRSS2* when TRIM25 was knocked out in both KO-1 and KO-2 cells compared to the non-targeted controls, confirming the findings from the RNA-seq analysis (Figure 3.5).

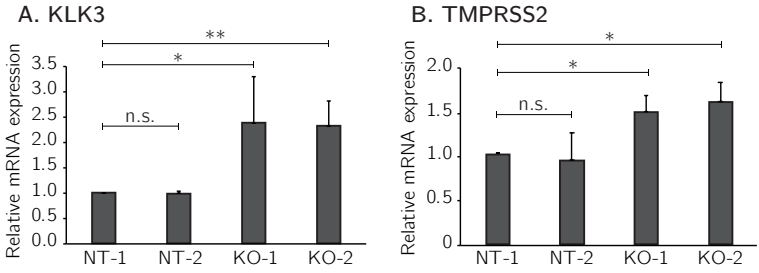

Figure 3.5: *KLK3* and *TMPRSS2* are upregulated upon TRIM25 knockout. LNCaP NT-1, NT-2, KO-1 and KO-2 cells were harvested and lysed. RNA was extracted, cDNAs were synthesized and qPCR was performed for *KLK3*, *TMPRSS2* and *GAPDH*. *KLK3* (**A**) and *TMPRSS2* (**B**) expression was normalized to the levels of GAPDH. The values for NT-1 cells were set to 1. Mean values and standard deviations were calculated from three independent experiments. Statistical analysis was performed using one-way ANOVA followed by Tukey's post hoc test. * = p-value < 0.05, ** = p-value < 0.01, n.s. = not significant.

3.2 TRIM25 controls KLK3/PSA levels

To determine if TRIM25 knockout influenced the regulation of these genes in an androgen-dependent or androgen-independent manner, LNCaP NT-1, NT-2, KO-1 and KO-2 cells were starved for 72 hours followed by treatment with 10 nM DHT or with the vehicle ethanol for 16 hours.

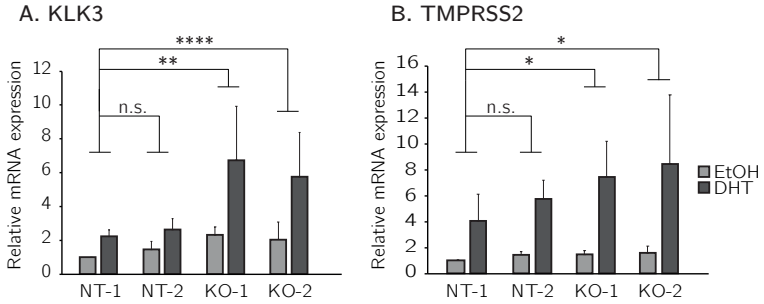

Figure 3.6: *KLK3* and *TMPRSS2* are upregulated upon TRIM25 knockout in an andorgen-dependent manner. NT-1, NT-2, KO-1 and KO-2 cells were starved for 72 hours and subsequently treated with 10 nM DHT or with vehicle ethanol (EtOH) for 16 hours. RNA was extracted, cDNAs were synthesized and RT-qPCR was performed for *KLK3*, *TMPRSS2* and *GAPDH*. The levels of *KLK3* (**A**) and *TMPRSS2* (**B**) were normalized to the levels of *GAPDH*. The values for NT-1 cells receiving ethanol were set to 1. Mean values and standard deviations were calculated from six independent experiments. Statistical analysis was performed using two-way ANOVA followed by Tukey's post hoc test to determine significant differences between the groups. * = p-value < 0.05, ** = p-value < 0.01, **** = p-value < 0.0001, n.s. = not significant.

The RT-qPCR results show that knocking out TRIM25 led to a significant increase of the mRNA levels of *KLK3* and *TMPRSS2* in an androgen-dependent manner (Figure 3.5B). Notably, the levels of *KLK3* expression were upregulated also without hormone addition, in KO-1 and KO-2 compared to NT-1 cells. This suggests that the effect of TRIM25 may also occur independently of hormone activation. These results provide further support to the previous findings that TRIM25 regulates *KLK3* and *TMPRSS2* expression (Figure 3.5) and suggest that TRIM25 controls at least *KLK3* in an androgen-dependent and potentially androgen-independent manners.

To explore whether the impact of TRIM25 on the AR response and KLK3 levels could also be observed at the protein level, mass-spectrometry analysis was conducted on NT-1 and TRIM25 knockout (KO-1 and KO-2) LNCaP cells. Cells were seeded and cultured until they reached 80% confluence before being harvested and sent for mass-spectrometry analysis. The obtained label-free quantitation (LFQ) intensities for all samples were utilized to calculate fold changes and p-values for

the comparison between KO-1 and NT as well as KO-2 and NT. These values were then visualized in volcano plots.

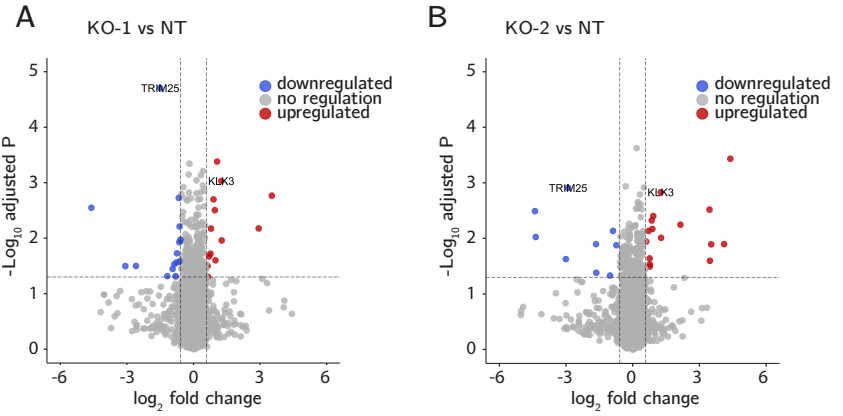

Figure 3.7: TRIM25 knockout upregulates KLK3 protein. Non-target (NT) and knockout (KO-1 and KO-2) cells were harvested and submitted for mass-spectrometry. The $\log_2$-transformed label-free quantitation (LFQ) intensities were utilized to calculate fold changes and p-values and volcano plots were generated. Graphs show $\log_2$ fold change values of the difference between KO-1 and NT (**A**) and KO-2 and NT (**B**) on the x-axis, and $-\log_{10}$ p-values on the y-axis. Proteins with a fold change greater than or equal to 1.5 (absolute value) and a p-value less than 0.05 were significantly regulated. Red dots represent proteins that were upregulated in TRIM25 knockout, while blue dots represent proteins that were downregulated.

The volcano plots illustrate that the knockout of TRIM25 altered protein levels. However, the number of regulated proteins was rather small compared to the number of altered transcripts observed after RNA-sequencing. Of note, KLK3 was again significantly upregulated in the TRIM25 knockout cell lines. This finding provides compelling evidence for the involvement of TRIM25 in the regulation of AR-mediated transcriptional response and particularly of KLK3 (Figure 3.7).

GSEA was performed on the mass-spectrometry data sets to identify changes in the activation of gene sets related to the AR pathway. The analysis revealed that the Hallmark Androgen Response gene set exhibited the most significant activation

in both KO-1 and KO-2 compared to NT (Figure 3.8A and 3.8B). This further supports the crucial role of TRIM25 in regulating the AR pathway.

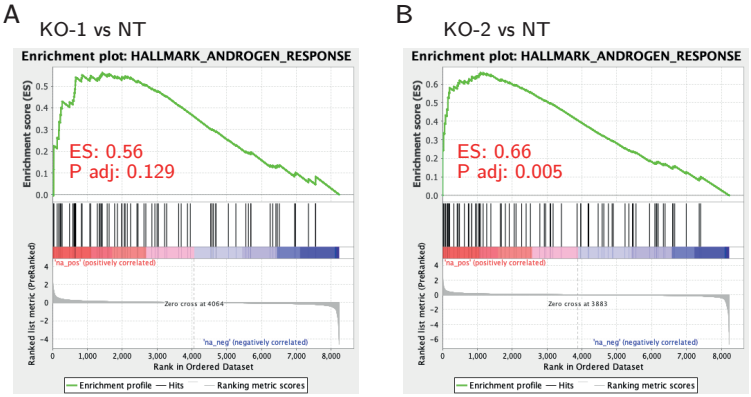

Figure 3.8: The Hallmark Androgen Response is activated upon TRIM25 knockout. After mass-spectrometry analysis, the fold changes derived from the comparison between KO-1 and NT, and KO-2 and NT were uploaded into the GSEA software. GSEA analysis was performed on the Hallmark signature. Displayed are enrichment plots showing the GSEA results for the Hallmark Androgen Response pathway in KO-1 vs NT (**C**), and KO-2 vs NT (**B**). The plots demonstrate the enrichment score (ES), with positive values indicating upregulation of the pathway in TRIM25 knockout cells, and the adjusted p-values (P adj).

The study observed modulation of the protein KLK3 levels resulting when TRIM25 was knocked out was further validated by Western blotting. After harvesting and lysing the cells, Western blotting was performed. Figure 3.9A shows that the levels of KLK3 protein were found to be strongly increased when TRIM25 was knocked out compared to the control samples, thus confirming the findings of the mass-spectrometry data (Figure 3.9A).

To study whether the induction of KLK3 when TRIM25 was knocked out depended on AR activation, cells were starved for 72 hours by culturing them in phenol red-free medium that was supplemented with CSS. Thereafter, the cells were treated with 10 nM DHT or the vehicle ethanol for 16 hours.

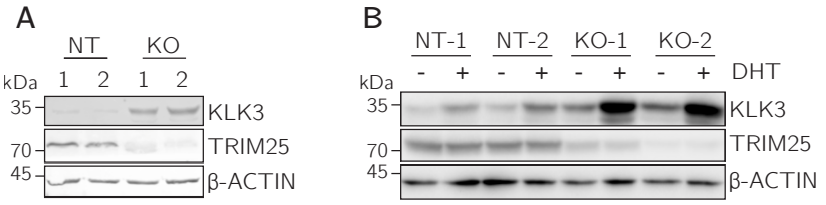

Figure 3.9: KLK3 is upregulated in LNCaP cells when TRIM25 is knocked out. (**A**) NT-1, NT-2, KO-1 and KO-2 LNCaP cells were harvested. Protein lysate was prepared, separated by an SDS-PAGE gel and blotted. The amounts of KLK3, TRIM25 and β-actin were monitored by incubating the membranes with the respective antibodies. (**B**) NT-1, NT-2, KO-1 and KO-2 LNCaP cells were cultured for 72 hours in phenol red-free medium supplemented with CSS. Thereafter, cells were treated with 10 nM DHT or the vehicle ethanol for 16 hours. Protein lysates were prepared, separated by gel electrophoresis, transferred onto a membrane, and probed with antibodies against KLK3, TRIM25 and β-actin, for loading control. Representative images of 3 independent experiments are shown.

Consistent with the induction of KLK3 mRNA, KLK3 protein levels were increased when TRIM25 was knocked out. This induction was even more pronounced when cells were treated wth DHT (Figure 3.9B).

The induction of KLK3 in the absence of hormone suggested at first an androgen-independent effect. However, the presence of low levels of hormones even in the charcoal-stripped FBS could not be totally excluded and thus AR could be slightly activated. Therefore, cells were treated with the AR inhibitor enzalutamide, harvested and analysed for KLK3 mRNA and protein levels by RT-qPCR and Western blotting, respectively. In line with the observed induction of KLK3 when no hormone was added (Figures 3.5 and 3.9), treating cells with enzalutamide did not completely abolish the induction of KLK3 when TRIM25 was knocked out (Figure 3.10). Taken together, these data suggest that TRIM25 may control KLK3 levels in an AR-dependent and AR-independent manner.

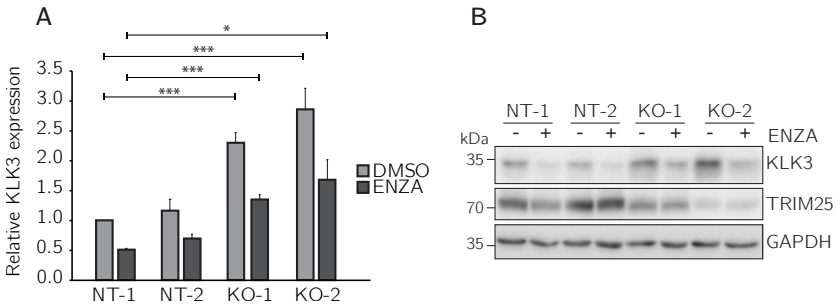

Figure 3.10: Treatment with enzalutamide does not prevent the induction of KLK3 when TRIM25 is knocked out. NT-1, NT-2, KO-1 and KO-2 LNCaP cells were treated with 10 µM enzalutamide (ENZA) for 24 hours. (**A**) Cells were harvested and RNA was extracted. The RNA was transcribed into a cDNA and RT-qPCR was performed to monitor KLK3 and GAPDH mRNA levels. Relative levels of KLK3 mRNA were determined by the $\Delta\Delta$Ct method. The values for NT cells that have received the vehicle DMSO were set to 1. Mean values and standard deviations of three independent experiments were calculated and plotted. Two-way ANOVA analysis followed by Tukey's test was applied for the statistical analysis. * = p-value < 0.05, *** p-value < 0.001. (**A**) NT-1, NT-2, KO-1 and KO-2 LNCaP cells were harvested and lysed. Cell lysates were separated by gel electrophoresis, transferred onto a membrane by Western blotting and the abundance of KLK3 was monitored by immunodetection. TRIM25 and GAPDH were immunodetected for control. The figure shows a representative image of 3 independent experiments.

The previous results (Figure 3.5A, Figure 3.6A, Figure 3.10A) show that TRIM25 affects KLK3 mRNA levels. This increase in KLK3 mRNA levels, when TRIM25 was knocked out could either result from increased transcription or from increased mRNA stability. To rule out an effect of TRIM25 on KLK3 mRNA stability, LNCaP cells were treated with actinomycin D to stop ongoing transcription. The decay of KLK3 mRNA was then monitored by RT-qPCR in TRIM25 knockout and non-targeted cells.

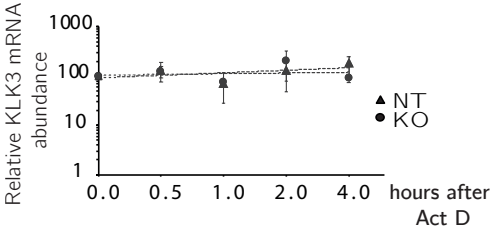

Figure 3.11: TRIM25 does not affect KLK3 mRNA stability. LNCaP NT and KO cells were treated with actinomycin D (Act D, 5 µg/ml) to inhibit transcription. Cells were harvested at the indicated time, RNA was prepared, transcribed into cDNA and RT-qPCR was performed to measure *KLK3* and *GAPDH* levels. After analysis of the raw data with the $\Delta\Delta$Ct method, using GAPDH as normalization control, relative KLK3 mRNA levels were determined. The values at the time of the addition of actinomycin D were set to 100. Mean values and standard deviations were calculated from 5 independent experiments and blotted.

As shown in Figure 3.11, KLK3 mRNA was found to be stable for the observation time of four hours, with a half-life far beyond the observation period. Furthermore, the knockout of TRIM25 did not affect KLK3 mRNA stability (Figure 3.11). To ensure that transcription was indeed blocked under these conditions, the stability of c-myc mRNA was also monitored. It was observed that the application of actinomycin D at the specified concentration and duration effectively reduced the half-life of c-myc mRNA. Moreover, no discernible alteration in the decay of c-myc mRNA was observed when comparing the KO and NT cell lines (Figure A.2). The collected evidence indicates that, as TRIM25 does not affect KLK3 mRNA stability, it must increase KLK3 mRNA levels by stimulating *KLK3* gene transcription.

To further analyze by which means TRIM25 affects KLK3 levels, KLK3 protein stability was determined analogously with a cycloheximide (CHX) chase assay in non-targeted and TRIM25 knockout LNCaP cells. Cells were treated with CHX to inhibit protein synthesis and harvested at 0, 2, 4 and 8 hours after CHX addition. Cells were lysed and abundances of KLK3, TRIM25 and GAPDH for internal control were determined by Western blotting.

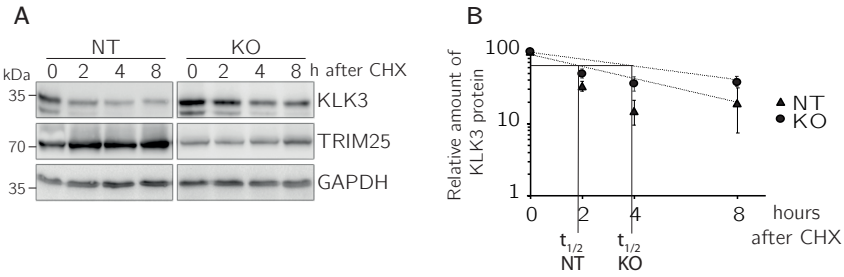

Figure 3.12: Deletion of TRIM25 leads to an increase in KLK3 protein half-life. (**A**) NT and KO LNCaP cells were treated with 20 µg/ml cycloheximide (CHX) and harvested at the indicated time. Protein lysates were prepared and analyzed for KLK3, TRIM25 and GAPDH by Western blotting. (**B**) The relative abundance of KLK3 was quantified. The values at the time of the addition of CHX were set to 100. Mean values and standard deviation of five independent experiments were calculated and plotted. The half-life ($t_{1/2}$) of KLK3 is indicated in the figure.

Figure 3.12 shows that knockout of TRIM25 resulted in a longer half-life of KLK3 compared to the non-targeted control. These data indicate that TRIM25 has a dual effect on KLK3 levels, by both controlling its transcription and by controlling its protein degradation.

3.3 Mechanisms of AR-mediated *KLK3* expression by TRIM25

The AR is a cytoplasmic receptor that translocates into the nucleus when activated by its ligand and binds to responsive elements in the promoters or enhancers of its target genes (Georget et al. 1997). Several steps form part of this activation and could potentially be perturbed by TRIM25, causing downstream effects on AR target genes expression. Some of these mechanisms, and whether they are perturbed by TRIM25, were investigated and are described in the following sections.

3.3.1 TRIM25 does not modify the expression of AR

Given that TRIM25 is known to be an E3 ligase involved in proteasomal degradation (Yang et al. 2022), it was investigated whether TRIM25 could affect AR abundance, which could in turn lead to changes in *KLK3* expression. To explore this possibility, the levels of AR protein were examined using both cells in which TRIM25 was knocked down via siRNA treatment (Figure 3.13A) and cells were TRIM25 was knocked out by CRISPR/Cas9 (Figure 3.13B).
Both in LNCaP cells were TRIM25 was downregulated by siRNA and in LNCaP cells were TRIM25 was knocked out by CRISPR/Cas9, no change was observed for AR levels (Figure 3.13).
Since the levels of AR protein remained unchanged when TRIM25 levels were modified, it can be concluded that the modulation of *KLK3* levels by TRIM25 does not occur through the modification of AR protein levels.

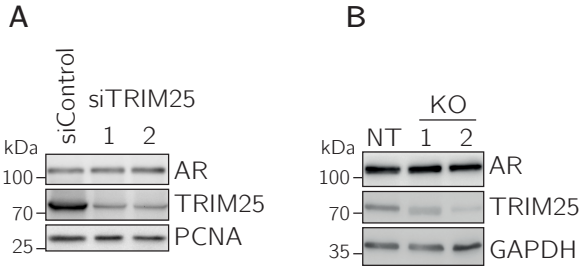

Figure 3.13: TRIM25 does not affect AR abundance. (**A**) 8 x 10^4 LNCaP cells were seeded into a well of a 24-well plate and transfected with 15 pmol of siRNA1 and siRNA2 both targeting TRIM25. A scrambled siRNA was transfected as control (siControl). 48 hours after transfection, cells were harvested and lysed. 45 µg of protein lysate were separated by SDS-PAGE and blotted onto a nitrocellulose membrane. AR, TRIM25 and PCNA protein levels were monitored by immunodetection. (**B**) Non-targeted (NT) and TRIM25-knockout (KO-1, KO-2) LNCaP cells were harvested and lysed. 45 µg of protein lysate were separated by SDS-PAGE and blotted onto a nitrocellulose membrane. AR, TRIM25 and GAPDH protein levels were monitored by immunodetection.

3.3.2 TRIM25 does not modify the subcellular localization of AR

To exert its transcriptional activity, the AR needs to translocate into the nucleus (Georget et al. 1997). Therefore, the impact of TRIM25 on AR subcellular localization was investigated, as higher nuclear levels of AR could potentially result in increased expression of *KLK3*.

To assess the impact of TRIM25 on the cellular localization of AR, non-targeted and TRIM25 knockout LNCaP cells were starved for 72 hours and subsequently treated with DHT for 4 hours. Cells were harvested and fractionated into cytoplasmic and nuclear fractions. Sonication was employed to enrich the nuclear fraction with proteins that are bound to chromatin. The levels of AR were then monitored by Western blotting.

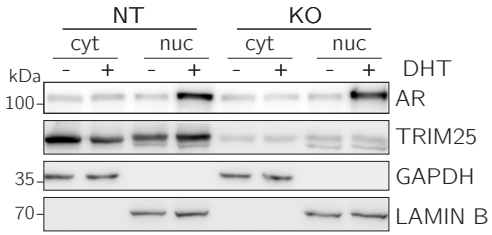

Figure 3.14: TRIM25 does not affect cellular localization of AR. NT and TRIM25-KO LNCaP cells were starved for 72 hours, treated with 10 nM DHT or with the vehicle ethanol for 4 hours and harvested. Cytoplasmic and nuclear fractions were prepared and the lysates were run on an SDS-PAGE gel. Western blotting was performed and the abundances of AR and TRIM25 were detected. GAPDH levels were monitored as cytoplasmic marker and Lamin B levels as nuclear marker. Shown is a representative image of 3 independent experiments.

As determined by V. Georget and colleagues, nuclear abundance of AR was increased when LNCaP cells were treated with DHT, showing the translocation of AR from the cytoplasm into the nucleus (Georget et al. 1997). This translocation occurred to the same level when TRIM25 was knocked out, demonstrating that TRIM25 did not affect the translocation of AR into the nucleus (Figure 3.14).

KLK3 expression is therefore not mediated through modulation of AR subcellular localization.

3.3.3 TRIM25 modifies the binding of AR to the chromatin

Once in the nucleus, AR binds as a dimer to AREs upstream of its target genes (Heinlein & Chang 2004). Therefore, the impact of TRIM25 on binding of AR to the enhancer region of the *KLK3* gene was investigated. Non-targeted and TRIM25 knockout LNCaP cells were starved for 72 hours followed by treatment with DHT for 4 hours. Cells were fixed and harvested for chromatin immunoprecipitation (ChIP) followed by quantitative PCR (qPCR). For qPCR analysis, two sets of primers were used for the AREIII region within the enhancer region of the *KLK3* gene. Additionally, primers targeting a region where AR does not bind were used as a normalization control.

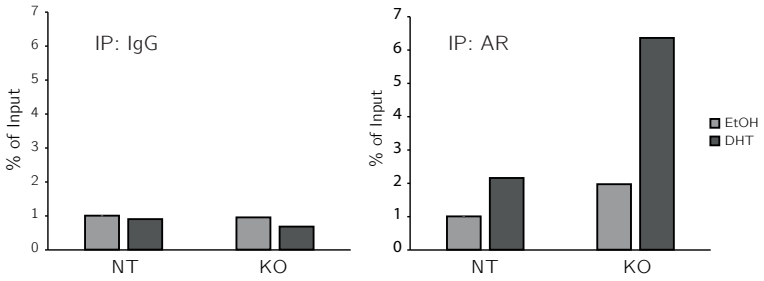

Figure 3.15: TRIM25 enhances AR binding to the *KLK3* enhancer region. Non-target (NT) and knockout (KO) cells were starved for 72 hours and treated with 10 nM DHT or with the vehicle ethanol (EtOH) for 4 hours. Cells were fixed with 1% formaldehyde at room temperature for 10 minutes and quenched with glycin. After washing with ice-cold PBS, cells were collected and lysed, and chromatin was sheared by sonication into fragments ranging from 200 to 500 bp. After overnight incubation with protein A agarose beads coupled to an antibody raised against AR or to IgG, the DNA fragments were eluted and employed for qPCR using primers for the AREIII region on the *KLK3* enhancer and primers for the reference sequence on *KIAA0066*. To analyse the data, the Ct value of the ChIP sample was first normalized by the Ct value of the input, and then further normalized with the values obtained for *KIAA0066*, used as internal control. The values for the non targeted cells that have been treated with ethanol were set to 1. The plots show the result of two experiments.

Figure 3.15 shows that the binding of AR to the AREIII on the *KLK3* enhancer is stronger when cells were treated with DHT, which is consistent with the expected response of AR to androgen stimulation (Heinlein & Chang 2004). Interestingly, when TRIM25 is knocked out, the binding of AR to the AREIII on the *KLK3* enhancer is increased, and even stronger when the cells are additionally treated with DHT, indicating an additive effect of TRIM25 knockout and DHT treatment (Figure 3.15). To provide additional support for this result, a second pair of primers targeting the same AR binding region were employed. Also with these primers, increased binding of AR to the *KLK3* enhancer could be observed when TRIM25 was knocked out (Appendix Figure A.3).

After having found that knocking out TRIM25 enhanced the binding of AR to chromatin, it was investigated whether TRIM25 could also bind to DNA and enhance the binding of AR to the enhancer directly at the DNA. This possibility seemed particularly likely as a previous report showed the interaction of TRIM25 with DNA in the promoter region of genes involved in proliferation, migration and hormone signalling in breast cancer cell lines (Walsh et al. 2017). To explore whether TRIM25 binds to DNA also in the LNCaP cell line, chromatin immunoprecipitation followed by sequencing (ChIP-seq) was performed.

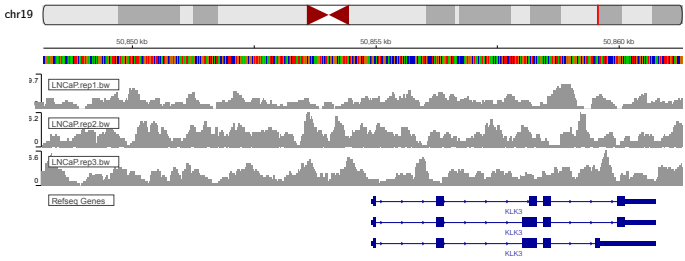

Figure 3.16: TRIM25 does not to DNA in LNCaP cells. LNCaP cells were cross-linked with 1% formaldehyde at room temperature for 10 minutes and quenched with glycin. After washing with ice-cold PBS, cells were collected and lysed, and chromatin was sheared by sonication. After overnight incubation with protein G agarose beads coupled to an antibody raised against TRIM25, the DNA fragments were eluted, purified and sent to the NKI Genomics Core facility in Amsterdam, for sequencing. The BigWig files obtained after the peak calling were uploaded onto the IGV (Integrative Genomics Viewer) software. The plot illustrates the shape and size of the peaks obtained from the ChIP-seq data around the *KLK3* gene on chromosome 19. The x-axis represents the genomic coordinates, while the y-axis represents the signal intensity.

LNCaP cells were lysed, and the chromatin was sheared by sonication, followed by immunoprecipitation of TRIM25. The DNA bound to TRIM25 was then sent for sequencing to the NKI Genomics Core facility in Amsterdam. Input samples were isolated before the immunoprecipitation step and used for normalization. After analysis of the data and peak calling, the resulting BigWig files were uploaded onto the Integrative Genomic Viewer (IGV) software to visualize the peaks across the genome. Specific attention was given to TRIM25 ChIP-seq peaks in proximity to the *KLK3* gene located on chromosome 19. However, the visualization depicted in Figure 3.16 shows that TRIM25 does not bind to the DNA around the *KLK3* locus (Figure 3.16). Furthermore, no binding of TRIM25 was observed throughout the entire genome (data not shown). Consequently, this comprehensive view provides compelling evidence that TRIM25 does not engage in DNA binding at all in LNCaP cells. As a result, it can be concluded that TRIM25 does not modulate *KLK3* expression by directly interacting with its promoter/enhancer region.

3.4 Regulation of p300 by TRIM25

Binding of AR to its binding sites on the DNA profoundly depends on coactivators and corepressors. Different coregulators operate with the AR to facilitate/impede its recruitment to those loci on the DNA (Heinlein & Chang 2002). One of the major AR co-factors is p300. p300 enhances AR-mediated transcriptional activation by promoting its recruitment to androgen-responsive genes and by stabilizing the transcriptional complex (Fu et al. 2000).

We have previously observed that TRIM25 controls p300 levels (Pauletto et al. in revision). Knockdown and knockout of TRIM25 in different cell lines and mouse embryonic fibroblasts resulted in upregulation of p300 protein levels and increased p300 activity. To see whether the regulation of p300 by TRIM25 occurs also in PCa cells, p300 levels were monitored in LNCaP cells where TRIM25 was knocked out and in non-targeted controls.
In contrast to H1299 cells, MCF7 cells and mouse embryonic fibroblasts (Pauletto et al. in revision), the amount of p300 protein was not enhanced in LNCaP cells when TRIM25 was knocked out (Figure 3.17A).

However, the activity of AR and its influence by TRIM25 and p300 was assessed with a dual reporter assay. H1299 cells were transfected with plasmids encoding AR, TRIM25, p300, a reporter where the MMTV promoter was fused to the firefly luciferase gene, and renilla luciferase, with the latter used as a normalization control. The cells were seeded and starved in phenol red-free DMEM culture medium, supplemented with 3 % CSS for 48 hours. The cells were then treated with either 10 nM DHT or with the vehicle ethanol for 24 hours, and finally harvested and lysed for dual reporter assay.

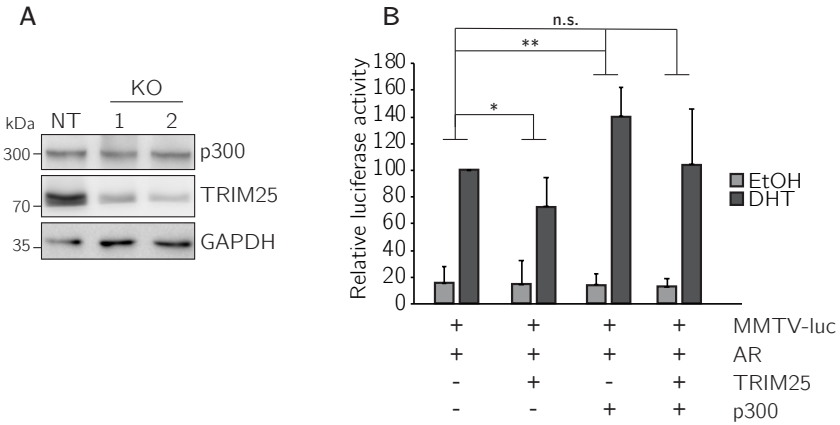

Figure 3.17: TRIM25 reverts p300-mediated induction of AR activity. (**A**) LNCaP NT, KO-1 and KO-2 cells were harvested and lysed. 45 µg of lysate were separated by SDS-PAGE and tranferred onto a nitrocellulose membrane. p300, TRIM25 and GAPDH, for loading control, protein levels were immunodetected. The figure shows a representative image of three independent experiments. (**B**) H1299 cells were transfected with plasmids encoding AR, TRIM25, p300, MMTV-firefly luciferase and Renilla luciferase, for internal control. After starving the cells for 48 hours, cells were treated with 10 nM DHT, where indicated, or with the vehicle ethanol. 24 hours after hormone addition, cells were lysed and a dual reporter assay was performed. The absorbance values obtained for the firefly luciferase were normalized with the values of the renilla luciferase. The luciferase activity when AR was overexpressed and cells were treated with DHT was set to 100. The graph shows mean values and standard deviations of five independent experiments. p-values were calculated using two-way ANOVA followed by Tukey's test. * = p-value < 0.05, ** = p-value < 0.01, n.s = not significant.

The results of the dual reporter assay show that overexpression of TRIM25 reduced AR activity on the MMTV promoter and overexpression of p300 increased its

activity. Moreover, the decrease of AR activity when TRIM25 was overexpressed was reversed by the overexpression of p300 (Figure 3.17B). These data suggest that the effect of TRIM25 on AR activity is at least in part mediated by p300.

To further investigate this, LNCaP cells were treated with the p300 inhibitor CCS1477 (Welti et al. 2021). First, NT, KO-1 and KO-2 LNCaP cells were starved for 72 hours. Then DHT was added to the cells. One hour prior to the treatment with DHT, part of the cells were treated with the p300 inhibitor while the remaining cells received the vehicle DMSO. 16 hours after hormone treatment, cells were lysed. RNA was prepared, transcribed into a cDNA and analysed by RT-qPCR.

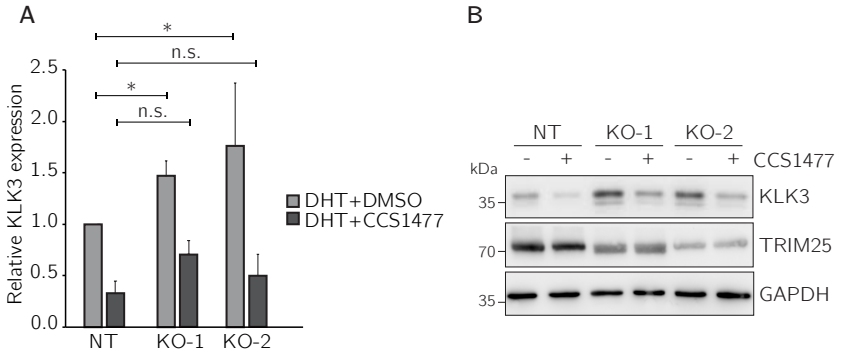

Figure 3.18: Inhibition of p300 reduces the effect of TRIM25 knockout on KLK3 expression. (**A**) NT, KO-1 and KO-2 LNCaP cells were starved for 72 hours and then treated with 10 nM DHT. One hour prior to DHT addition, 100 nM CCS1477 or the vehicle DMSO were added to the cells where indicated. 16 h after hormone treatment, cells were lysed. RNA was prepared, transcribed into cDNA and KLK3 and actin RNA levels were monitored by RT-qPCR. Mean values and standard deviations were calculated from 5 independent experiments and plotted. The value for cells treated only with DHT was set to 1. p-values were calculated using two-way ANOVA followed by Tukey's test. * = p-value < 0.05, n.s. = not significant.(**B**) NT, KO-1 and KO-2 LNCaP cells were starved for 72 hours and then treated with 10 nM DHT. One hour prior to DHT addition, 100 nM CCS1477 or the vehicle DMSO were added to the cells where indicated. 16 hours after hormone treatment, cells were harvested and lysed. 45 µg protein lysate were separated on an SDS-PAGE gel and transferred onto a nitrocellulose membrane. The levels of KLK3, TRIM25 and GAPDH, used for loading control, were immunodetected by Western blotting. A representative image of 2 independent experiments is shown.

As shown before (Figure 3.5A, Figure 3.6A, Figure 3.9), KLK3 levels were significantly elevated when TRIM25 was knocked out. This increase in KLK3 levels was strongly reduced when the cells were pre-treated with the p300 inhibitor. Although there was still a tendency towards higher *KLK3* expression in the TRIM25 knockout cells, the values did not reach statistical significance anymore (Figure 3.18A). The analysis of KLK3 protein levels mirrored the RT-qPCR data. KLK3 protein levels were clearly reduced when p300 was inhibited confirming earlier results that showed that KLK3 expression is regulated by p300 (Welti et al. 2021), while there was still a tendency towards higher KLK3 expression when TRIM25 was knocked out (Figure 3.18B). Whether this increased expression is due to incomplete inhibition of p300 or to the AR-independent mode of KLK3 regulation remains to be determined.

3.5 Proliferation of LNCaP cells is increased upon TRIM25 knockdown

Increased AR activity and increased KLK3 levels are correlated to a higher proliferation rate in prostate cells ((Shim & Cohen 1999, Niu et al. 2008, Xu et al. 2006)). On the other hand, TRIM25 has been shown to have a pro-proliferative and pro-oncogenic effect of TRIM25 in PCa and PCa cells (Takayama et al. 2018, Wang et al. 2016, Li et al. 2022), which is contradictory with its ability to inhibit the AR signalling and KLK3 expression that is shown in this work.
LNCaP cells were infected with lentivirus carrying a shRNA targeting TRIM25 (shTRIM25) or a shRNA for control (shControl). After selection for infected cells to obtain stable cell lines, the knockdown of TRIM25 was validated by Western blotting. As shown in Figure 3.19A, the infection of LNCaP cells with lentivirus carrying shRNA against TRIM25 resulted in a clear downregulation of TRIM25 (Figure 3.19A).
For proliferation analysis, shControl and shTRIM25 cells were seeded into a 24-well plate and counted for four consecutive days. The downregulation of TRIM25 resulted in a significant increase in proliferation of LNCaP cells, compared to the non-targeted control (Figure 3.19B).

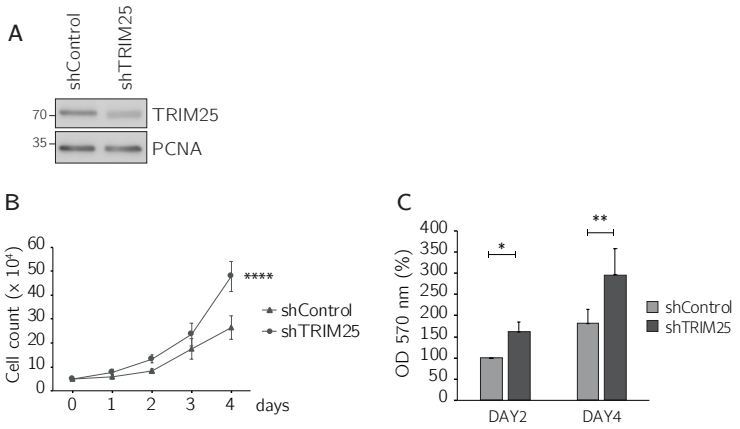

Figure 3.19: TRIM25 knockdown increases the proliferation of LNCaP cells. LNCaP cells were infected with lentiviruses carrying a shRNA for TRIM25 (shTRIM25) or a scrambled shRNA as control (shControl). (**A**) shControl and shTRIM25 cells were harvested and lysed. 45 µg of lysate were separated by SDS-PAGE and transferred onto a nitrocellulose membrane. TRIM25 and PCNA, for loading control, protein levels were immunodetected. The figure shows a representative image of three independent experiments. (**B**) 5 x 10^4 cells were plated per well of a 24-well plate. Cells were trypsinazed and counted every day for 4 days. Mean values and standard deviations of 4 independent experiments were calculated and plotted. The p-value was calculated with Student's t test. **** = p-value < 0.0001. (**C**) 3 x 10^3 cells were seeded per well of a 96-well plate and incubated. 2 and 4 days after seeding, MTT solution was added to the cells and the cells were incubated until the formation of fromazan crystals was clearly visible. After that, the crystals were dissolved in isoprapanol and the absorbance of the solution was measured at 590 nm. The absorbance values of the shControl at day 2 was set to 100. The bar plot represents mean values and standard deviations of 3 independent experiments. The p-values were calculated using two-way ANOVA followed by Tukey's test. * = p-value < 0.05, ** = p-value < 0.01.

To confirm these data, MTT assays were performed. shTRIM25 and shControl cells were cultured for 2 or 4 days. Then, MTT was added to the cells until the formation of purple crystals was observed. The crystals were dissolved in isopropanol and intensity of the purple colour was monitored. Figure 3.19C shows that knocking down TRIM25 significantly increased the optical density of the formazan solution at day 2 and 4, which is correlated to a higher capacity of the cells to metabolize the MTT, which is in turn correlated with a higher number of living cells (Figure 3.19C). These results indicate that TRIM25 modulates cell proliferation in the LNCaP cells.

4 Discussion

Prostate cancer (PCa) is a prevalent malignancy and a leading cause of cancer-related deaths in men worldwide (Sung et al. 2021). The progression and development of PCa are largely driven by the androgen receptor (AR) signalling pathway, making AR an attractive therapeutic target (Huggins et al. 1941). Current treatment approaches predominantly involve the use of drugs that directly inhibit AR activity or androgen synthesis (Evans 2018). However, the clinical efficacy of these treatments is often limited due to the emergence of resistance mechanisms against these drugs, leading to disease relapse and progression (Scher et al. 2012, Beer et al. 2014). In recent years, there has been a growing interest in exploring alternative strategies to enhance the effectiveness of AR-targeted therapies in PCa. One approach involves targeting the coregulators of AR, which are proteins that interact with AR and modulate its transcriptional activity. These coregulators play crucial roles in AR-mediated gene expression and are essential for maintaining the oncogenic potential of AR signalling in PCa (Heinlein & Chang 2002). A promising strategy involves inhibiting p300, a crucial protein that interacts with AR and plays a pivotal role in regulating its transcriptional activity, as well as exerting influence on global transcription through histone acetylation. In preclinical studies, the p300 inhibitor CCS1477 has demonstrated encouraging anti-tumour effects by reducing the recruitment of CBP, p300 and AR to AR binding sites, so that it is now tested in clinical trials for the treatment of advanced PCa (Welti et al. 2021).

TRIM25 is a key player in the regulation of protein degradation, an E3 ubiquitin ligase that has shown increased expression in PCa specimens compared to healthy tissues (Wang et al. 2016). Moreover, its expression has been correlated with high Gleason scores in PCa (Li et al. 2022), indicating its potential significance in disease progression. Although various mechanisms have been proposed to

elucidate how TRIM25 controls PCa growth, such as reducing apoptosis through decreased p53 activity or enhancing glucose metabolism in PCa cells (Takayama et al. 2018, Li et al. 2022), its involvement in regulating AR signalling remains understudied. This study aimed to investigate the role of TRIM25 in controlling AR signalling, particularly as our group has found that TRIM25 interacts with and targets p300 for degradation (Pauletto et al. in revision). This result suggested that TRIM25 might also modulate AR signalling via controlling p300 levels and activity.

4.1 TRIM25 modulates AR activity and KLK3 levels

The initial findings that TRIM25 overexpression reduced AR activity on the MMTV promoter was further explored by assessing the global changes in gene expression by RNA sequencing of LNCaP cells where TRIM25 was knocked out. Gene Set Enrichment Analysis (GSEA) demonstrated a significant activation of the androgen response in the TRIM25 knockout cells compared to the control group. This activation suggests that the loss of TRIM25 may lead to a general increase in AR signalling in LNCaP cells. Furthermore, a significant induction of *KLK3* and *TMPRSS2* expression, two well-known target genes of AR (Jin et al. 2013), was seen in LNCaP cells when TRIM25 was knocked out and cells were treated with DHT. This finding indicates that TRIM25 controls the expression of these genes in an androgen-dependent manner. Notably, for *KLK3*, there was also an induction observed without DHT addition when TRIM25 was knocked out, suggesting that TRIM25 may regulate this gene also in an androgen-independent manner as well. Altogether, these findings provide direct evidence that TRIM25 plays a role in modulating the expression of AR target genes in PCa cells.
In addition to the RNA-seq analysis, mass spectrometry-based proteomic profiling was performed. The number of proteins regulated by TRIM25 knockout was comparatively smaller than the number of regulated transcripts identified by RNA-sequencing. However, 25% of the proteins exhibiting TRIM25-dependent

regulation in the mass spectrometry analysis were also found to be significantly regulated in the RNA-seq analysis. This subset of proteins demonstrated consistent and statistically significant changes in expression levels at both the protein and transcript levels. To explain the little overlap between transcriptomic and proteomic data, it is plausible to consider that TRIM25 primarily influences gene expression at the transcriptional level, leading to substantial changes in mRNA abundance. However, it is also possible that post-transcriptional and post-translational regulatory mechanisms contribute to the observed proteomic alterations, resulting in a more modest overlap with the transcriptomic data.

One of the genes that showed consistent upregulation both in the RNA-seq results and in the mass spectrometry dataset was *KLK3*. This concordance between transcriptomic and proteomic analyses provides robust evidence for the modulation of KLK3 expression by TRIM25 in LNCaP cells. Also when the mass spectrometry and RNA-seq data were validated by Western blotting and RT-qPCR analysis, KLK3 mRNA and protein was induced when TRIM25 was knocked out, both in the presence and in the absence of DHT. Importantly, the observed upregulation of KLK3 in both the DHT-treated and vehicle-treated conditions suggests again that TRIM25 may control KLK3 expression in an androgen-dependent as well as in an androgen-independent manner.

To further investigate the nature of the regulation of KLK3 expression by TRIM25, cells were treated with enzalutamide, an AR inhibitor. Surprisingly, even in the presence of enzalutamide, increasing levels of KLK3 were still observed when TRIM25 was knocked out. This result suggests that TRIM25's control of KLK3 expression extends beyond its influence on AR signalling and indicates the involvement of alternative pathways that can be used by TRIM25 to regulate *KLK3* expression. It is possible that TRIM25 interacts with other transcriptional regulators or influences signalling pathways independently of AR.

In order to further elucidate the regulatory mechanisms involved in TRIM25-mediated *KLK3* expression, additional experiments were conducted. Treatment of the cells with actinomycin D, a transcriptional inhibitor, revealed that the stability of the KLK3 mRNA was not affected by TRIM25, indicating that TRIM25 rather modulates *KLK3* transcription. In contrast, treatment of the cells with cycloheximide, a protein synthesis inhibitor, demonstrated a noticeable stabilization

of KLK3 protein when TRIM25 was knocked out compared to the control group. This indicates that TRIM25 may play a role in modulating the degradation or turnover of KLK3 protein, a mechanism that was not further examined in this study.

4.2 TRIM25 controls KLK3 expression by modulating the binding of AR to its enhancer region

TRIM25 is mostly recognized for its ability to mediate the degradation of specific proteins via ubiquitination, thereby exerting control over their cellular abundance (Yang et al. 2022). Given this characteristic, the possibility of TRIM25 influencing AR levels was explored by examining the effects of TRIM25 on AR protein expression. Contrary to the expectations, no substantial modifications in AR levels were observed upon TRIM25 silencing or knockout.

Another possibility by which TRIM25 could affect AR activity is by changing its subcellular localization. Normally, the AR is retained in the cytoplasm, by binding to heatshock proteins and other co-chaperones (Fang et al. 1996). Only after binding to hormone, the AR is released from its constraints and able to translocate into the nucleus via importin-α (Kaku et al. 2008). Therefore, it would be conceivable that TRIM25 affects AR activity by allowing controlling its translocation into the nucleus. The subcellular localization of the AR was assessed to investigate any potential changes in AR levels within the cytoplasm and nucleus. However, no significant alterations in AR levels were observed in either the cytoplasmic or nuclear fractions when comparing the TRIM25 knockout samples to the control group. These results suggest that TRIM25 does not have a direct impact on the cellular distribution or localization of AR in the experimental conditions examined.

After obtaining negative results regarding the effects of TRIM25 on AR protein levels and AR cellular localization, chromatin immunoprecipitation was performed to examine the binding of AR to the enhancer region of *KLK3* comparing

the TRIM25 knockout samples to the control group. The results of this experiment revealed that knocking out TRIM25 resulted in an increased binding of AR to the enhancer region of *KLK3*. Interestingly, this increased binding was observed even in the absence of DHT addition, suggesting that TRIM25 may enhance AR responsiveness under basal hormonal conditions.

The observation that TRIM25 knockout led to elevated levels of KLK3 mRNA and protein without DHT raises the possibility that TRIM25 sensitizes AR to low hormone levels. This heightened AR responsiveness given by the knockout of TRIM25 in the absence of DHT could potentially explain the increased binding of AR to the enhancer region of *KLK3* and the subsequent upregulation of *KLK3* expression. Yet, this raises the intriguing question about the underlying mechanism through which TRIM25 could achieve a better binding of AR to the ARE. One possibility would be that TRIM25, either directly or indirectly, modifies the conformation or recruitment of coactivators to AR, allowing it to be more sensitive to lower hormone concentrations. Alternatively, TRIM25 might be involved in post-translational modifications that enhance AR's DNA binding capacity and transcriptional activity. To confirm the hypothesis that the absence of TRIM25 makes AR more sensitive to low hormone concentrations, DHT titration experiments involving the exposure of cells to different concentrations of DHT, and subsequent analysis of AR target genes expression and AR DNA binding, should be performed.

One crucial aspect of gene regulation is the formation of chromatin loops between the promoter and enhancer regions of target genes, such as *KLK3* (Shang et al. 2002). Also, the AR transcriptional complex is assembled through a series of protein-protein interactions involving AR, coregulators, and other transcription factors (Heinlein & Chang 2002). This complex is responsible for initiating and regulating the transcription of target genes. During the initiation of transcription of AR target genes, AR binds to the enhancer region of e.g. *KLK3* and then interacts with its promoter region, mediated by other members of the complex. Disruption or alteration of this chromatin looping can have significant consequences on gene expression (Shang et al. 2002). TRIM25, as an E3 ligase, has the potential to modulate the formation of the AR transcriptional complex and

chromatin looping. It may do so by targeting specific components involved in the assembly or stabilization of this complex for ubiquitin-mediated degradation or by interfering with protein-protein interactions critical for complex formation. The dysregulation of chromatin looping between the *KLK3* promoter and enhancer regions due to TRIM25 dysfunction or depletion could result in changes in the gene expression pattern and could contribute to the dysregulated expression of *KLK3* expression when TRIM25 levels change.

4.3 TRIM25-dependent modulation of KLK3 occurs via p300 mediation

The formation of the AR transcriptional complex relies on the recruitment of coactivators such as p300, which facilitate the assembly of the complex at target gene loci. This assembly involves protein-protein interactions between AR, p300, and other coregulatory factors, leading to the activation of transcription (Shang et al. 2002). It has been observed that TRIM25 can induce the degradation of p300 in various cell lines (Pauletto et al. in revision). This finding suggests that TRIM25 may play a crucial role in modulating p300 levels, thus impacting its coactivator function and influencing AR activity. Despite TRIM25 not being found to affect p300 protein levels in LNCaP cells, the reporter assay assessing AR activity on the MMTV promoter revealed that p300 alters AR-mediated transcription, as shown before by M. Fu and colleagues (Fu et al. 2000). Moreover, overexpression of TRIM25 counteracted this effect by restoring AR activity levels to their initial state. To further investigate the role of p300 in the TRIM25-dependent modulation of KLK3 expression, LNCaP cells were treated with the p300 inhibitor CCS1477. The treatment of LNCaP cells with the p300 inhibitor reduced KLK3 expression, confirming the data shown by J. Welti and colleagues (Welti et al. 2021). Furthermore, inhibition of p300 combined with knockout of TRIM25 resulted in no significant changes in KLK3 mRNA levels, suggesting that TRIM25 knockout cannot efficiently induce *KLK3* levels when p300 activity is inhibited. Similar results were obtained when KLK3 protein levels were studied upon CCS1477 treatment. These observations indicate that TRIM25 may rely on

the presence of functional p300 to modulate *KLK3* expression.
The potential interplay between TRIM25, p300, and the transcriptional activity of AR presents an intriguing mechanism by which TRIM25 may influence the expression of *KLK3* in PCa. One possibility is that TRIM25 modulates p300 activity, which in turn affects the transcriptional activity of AR. p300, being a histone acetyltransferase (HAT), has the ability to modify chromatin structure by acetylating histone proteins. This acetylation process can lead to a more relaxed chromatin structure, allowing for enhanced accessibility of transcription factors to their target genes. In this context, TRIM25 may regulate p300 HAT activity, potentially targeting specific lysine residues on histones associated with the *KLK3* gene promoter region. By controlling the acetylation status of these histones, TRIM25 could influence the binding of AR to the *KLK3* enhancer and subsequently impact *KLK3* transcription. Alternatively, TRIM25 may modify the p300-mediated AR acetylation. These modifications could directly affect the transcriptional activity of AR by influencing its recruitment to regulatory regions of the *KLK3* gene.
Future studies utilizing advanced techniques such as chromatin immunoprecipitation and mass spectrometry-based proteomics hold promise in unraveling the precise mechanisms through which TRIM25 influences the interplay between p300, histones, and AR in regulating *KLK3* expression. Chromatin immunoprecipitation can provide valuable insights into the binding dynamics e.g. of p300 to specific DNA regions, shedding light on whether changes in TRIM25 levels could result in differential binding of p300 to its target sites. This approach can help decipher whether TRIM25 acts as a modulator of p300's recruitment to *KLK3* regulatory regions, ultimately impacting AR transcriptional activity. Additionally, mass spectrometry-based proteomics can offer a comprehensive analysis of post-translational modification of proteins, including histone and AR acetylation. By investigating the acetylation patterns in the presence or absence of TRIM25, it could be ascertained whether TRIM25 influences the acetylation status of histones and/or AR, potentially affecting their interactions and subsequent transcriptional regulation of *KLK3*.

4.4 TRIM25 inhibits the proliferation of LNCaP cells

Two previous publications reported stimulation of PCa cell proliferation by TRIM25 (Takayama et al. 2018, Wang et al. 2016). However, the present study found that TRIM25 decreased AR signalling and KLK3 levels, which are typically associated with cell proliferation in PCa (Shim & Cohen 1999, Niu et al. 2008, Xu et al. 2006). Thus, the results presented in this thesis contradicted the reported increase in cell proliferation. For this reason, the proliferation of LNCaP cells where TRIM25 was downregulated was examined. Consistent with the increase in AR activity and KLK3 levels, a higher proliferation rate of cells with downregulated TRIM25 was observed compared to control cells.

The discrepancy between the proliferation data obtained in the thesis study, involving stable shRNA knockdown of TRIM25 in LNCaP cells, and the published data on TRIM25 knockdown in LNCaP cells utilizing siRNA transient knockdown (Takayama et al. 2018), could be attributed to differences in the knockdown methods employed. Additionally, variations in the cellular context and potential compensatory mechanisms that are established during the stable knockdown may influence the observed effects. Alternatively, the LNCaP cell lines used in the different laboratories may possess intrinsic differences in the genetic background and signalling pathways, contributing to disparate responses to TRIM25 knockdown and subsequent cellular proliferation.

The controversy arising from patient data indicating a correlation between TRIM25, tumour growth and Gleason score (Wang et al. 2016, Li et al. 2022) highlights the need to also consider the complexities of the clinical context and the limitations of in vitro cell line studies. Patient data encompass a range of factors, including interactions with surrounding stromal cells, immune responses, and angiogenesis, which can modulate the impact of TRIM25 on tumour growth and Gleason score.

In conclusion, the discrepancy between the data obtained in the thesis study and the published data, as well as the controversy surrounding the correlation between TRIM25 and tumour growth in patient data, highlights the need for further

research to elucidate the role of TRIM25 in PCa and reconcile the observed discrepancies.

A Appendix Figures

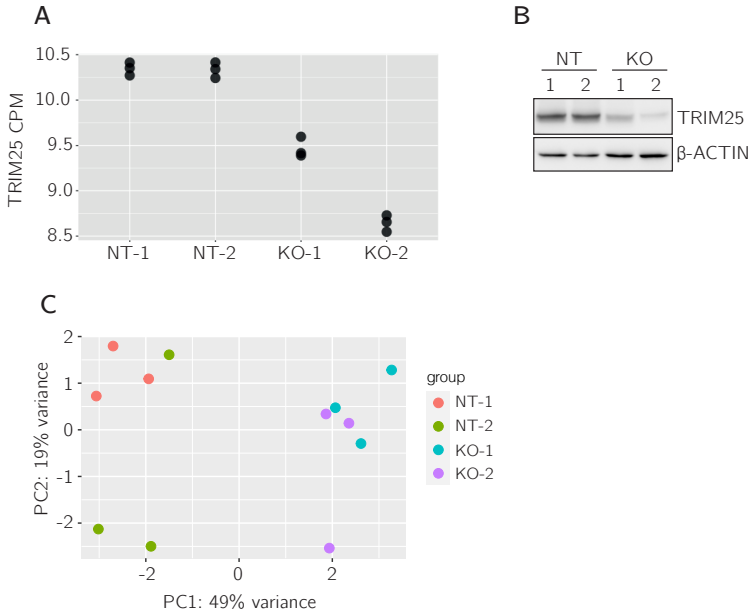

Figure A.1: TRIM25 levels are reduced in TRIM25 knockout LNCaP cell lines. LNCaP cells where TRIM25 was knocked out by CRISPR/Cas9 with two different guide RNAs (KO-1 and KO-2) were used for RNA-seq experiments. Two non-targeting sgRNAs were included as controls (NT-1 and NT-2). (**A**) Counts per million (CPM) values for all samples and replicates were plotted. (**B**) Cells were lysed and analysed for TRIM25 expression by Western blotting. Immunodetection of β-actin was performed for loading control. (**C**) Principal component analysis (PCA) plot illustrates the clustering and distribution of the different samples based on their gene expression profiles.

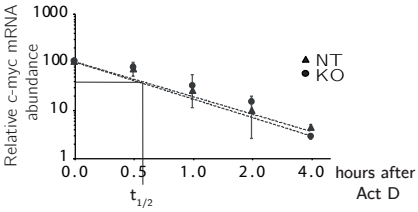

Figure A.2: Half-life of c-myc mRNA. LNCaP NT and KO cells were treated with actinomycin D (Act D, 5 µg/ml) and harvested at the indicated times. RNA was prepared, transcribed into cDNA and qPCR was performed to measure c-myc and GAPDH levels. The raw data were analyzed using the $\Delta\Delta$Ct method with normalization to GAPDH, and the mean values for each time point were calculated relative to the mean value at time point 0, which was set to 100. The graph shows mean values and standard deviations of 5 independent experiments.

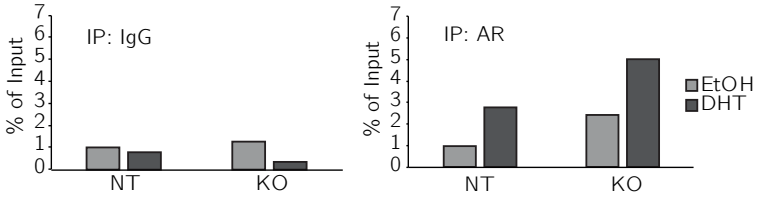

Figure A.3: TRIM25 knockout increases the binding of AR to the *KLK3* enhancer. LNCaP NT and KO cells were starved for 72 hours before they were treated with 10 nM DHT or with ethanol for 4 hours. Cells were fixed with 1% formaldehyde at room temperature for 10 minutes and quenched with glycine. After washing with ice-cold PBS, cells were collected and lysed, and chromatin was sheared by sonication. After overnight incubation with protein A agarose beads coupled to an antibody raised against AR (IP: AR) or IgG (IP: IgG), the DNA fragments were eluted and employed for qPCR using primers for the AREIII on the *KLK3* enhancer. The results were analysed with the percentage of input method, were the Ct values of AREIII were normalized to the Ct values of the input controls. The values obtained were further normalized to the values obtained for KIAA0066, the reference sequence. The plots show the mean values obtained after analysing two experiments.

List of Figures

List of Tables

List of Publications

Journal Articles

Pauletto, E., Eickhoff, N., Padrão, N. A., Blattner, C., Zwart, W. (2021), 'TRIM-ming down hormone-driven cancers: the biological impact of TRIM proteins on tumor development, progression and prognostication', *Cells* 10(6):1517.

Pauletto, E., Eickhoff, N., Padrão, N. A., Zwart, W., Blattner, C. (In revision), 'TRIM25 targets p300 for degradation.'

Conference Contributions

Posters

Pauletto, E., Blattner, C. 'Role of TRIM25 in prostate cancer', *MSCA cluster event on cancer research and innovation*, Online meeting, Mar 2021.

Pauletto, E., Eickhoff, N., Padrão, N. A., Blattner, C., Zwart, W., 'TRIM25 controls the AR signalling and PSA levels in prostate cancer.', *A 20/20 vision of the future of nuclear receptors 2022*, Sep 2022.

Talks

Pauletto, E., Blattner, C., 'Deciphering new targets in prostate cancer.', *Night of Science, Karlsruhe Institute of Technology*, Nov 2020.

Pauletto, E., Eickhoff, N., Padrão, N. A., Blattner, C., Zwart, W., 'TRIM25 controls the AR signalling and PSA levels in prostate cancer', *H2020-MSCA-ITN TRIM-NET, closure meeting*, Jun 2023.

Bibliography

Aarnisalo, P., Palvimo, J. J. & Jänne, O. A. (1998), 'Creb-binding protein in androgen receptor-mediated signaling', *Proceedings of the National Academy of Sciences* **95**(5), 2122–2127.

Adler, A. J., Scheller, A. & Robins, D. M. (1993), 'The stringency and magnitude of androgen-specific gene activation are combinatorial functions of receptor and nonreceptor binding site sequences', *Molecular and Cellular Biology* **13**(10), 6326–6335.

Beer, T. M., Armstrong, A. J., Rathkopf, D. E., Loriot, Y., Sternberg, C. N., Higano, C. S., Iversen, P., Bhattacharya, S., Carles, J., Chowdhury, S. et al. (2014), 'Enzalutamide in metastatic prostate cancer before chemotherapy', *New England Journal of Medicine* **371**(5), 424–433.

Bevan, C. L., Hoare, S., Claessens, F., Heery, D. M. & Parker, M. G. (1999), 'The af1 and af2 domains of the androgen receptor interact with distinct regions of src1', *Molecular and cellular biology* **19**(12), 8383–8392.

Blighe, K., Rana, S. & Lewis, M. (2019), 'Enhancedvolcano: Publication-ready volcano plots with enhanced colouring and labeling', *R package version* **1**(0).

Borgono, C. A., Michael, I. P. & Diamandis, E. P. (2004), 'Human tissue kallikreins: physiologic roles and applications in cancer', *Molecular cancer research* **2**(5), 257–280.

Bostwick, D. G. & Cheng, L. (2014), *Urologic Surgical Pathology*, 3rd edn, Elsevier.

Burris, T. P. & McCabe, E. R. (2000), *Nuclear receptors and genetic disease*, Academic Press.

Cancer Research UK (2023), 'Metastatic prostate cancer', https://www.cancerresearchuk.org/about-cancer/prostate-cancer/metastatic-cancer/what-is-metastatic-prostate-cancer. Accessed: June 1, 2023.

Carlson, M., Falcon, S., Pages, H., Li, N. et al. (2019), 'org. hs. eg. db: Genome wide annotation for human', *R package version* **3**(2), 3.

Chandrasekar, T., Yang, J. C., Gao, A. C. & Evans, C. P. (2015), 'Mechanisms of resistance in castration-resistant prostate cancer (crpc)', *Translational andrology and urology* **4**(3), 365.

Chen, M., Lingadahalli, S., Narwade, N., Lei, K. M. K., Liu, S., Zhao, Z., Zheng, Y., Lu, Q., Tang, A. H. N., Poon, T. C. W. et al. (2022), 'Trim33 drives prostate tumor growth by stabilizing androgen receptor from skp2-mediated degradation', *EMBO reports* **23**(8), e53468.

Chen, S., Gulla, S., Cai, C. & Balk, S. P. (2012), 'Androgen receptor serine 81 phosphorylation mediates chromatin binding and transcriptional activation', *Journal of Biological Chemistry* **287**(11), 8571–8583.

Cho, H., Orphanides, G., Sun, X., Yang, X.-J., Ogryzko, V., Lees, E., Nakatani, Y. & Reinberg, D. (1998), 'A human rna polymerase ii complex containing factors that modify chromatin structure', *Molecular and cellular biology* **18**(9), 5355–5363.

Claessens, F., Denayer, S., Tilborgh, N. V., Kerkhofs, S., Helsen, C. & Haelens, A. (2008), 'Diverse roles of androgen receptor (ar) domains in ar-mediated signaling', *Nuclear Receptor Signaling* **6**(1), nrs.06008.

Clegg, N. J., Wongvipat, J., Joseph, J. D., Tran, C., Ouk, S., Dilhas, A., Chen, Y., Grillot, K., Bischoff, E. D., Cai, L. et al. (2012), 'Arn-509: A novel antiandrogen for prostate cancer treatmentdevelopment of antiandrogen arn-509', *Cancer research* **72**(6), 1494–1503.

Cleutjens, K. B., van Eekelen, C. C., van der Korput, H. A., Brinkmann, A. O. & Trapman, J. (1996), 'Two androgen response regions cooperate in steroid

hormone regulated activity of the prostate-specific antigen promoter ()', *Journal of Biological Chemistry* **271**(11), 6379–6388.

Cumming, A., Hopmans, S., Vukmirović-Popović, S. & Duivenvoorden, W. (2011), 'Psa affects prostate cancer cell invasion in vitro and induces an osteoblastic phenotype in bone in vivo', *Prostate cancer and prostatic diseases* **14**(4), 286–294.

Debes, J. D., Schmidt, L. J., Huang, H. & Tindall, D. J. (2002), 'p300 mediates androgen-independent transactivation of the androgen receptor by interleukin 6', *Cancer research* **62**(20), 5632–5636.

Dehm, S. M., Schmidt, L. J., Heemers, H. V., Vessella, R. L. & Tindall, D. J. (2008), 'Splicing of a novel androgen receptor exon generates a constitutively active androgen receptor that mediates prostate cancer therapy resistance', *Cancer research* **68**(13), 5469–5477.

Doesburg, P., Kuil, C. W., Berrevoets, C. A., Steketee, K., Faber, P. W., Mulder, E., Brinkmann, A. O. & Trapman, J. (1997), 'Functional in vivo interaction between the amino-terminal, transactivation domain and the ligand binding domain of the androgen receptor', *Biochemistry* **36**(5), 1052–1064.

Duffy, M. J. (2020), 'Biomarkers for prostate cancer: prostate-specific antigen and beyond', *Clinical Chemistry and Laboratory Medicine (CCLM)* **58**(3), 326–339.

Evans, A. J. (2018), 'Treatment effects in prostate cancer', *Modern Pathology* **31**, 110–121.

Fang, Y., Fliss, A. E., Robins, D. M. & Caplan, A. J. (1996), 'Hsp90 regulates androgen receptor hormone binding affinity in vivo', *Journal of Biological Chemistry* **271**(45), 28697–28702.

Fong, K.-w., Zhao, J. C., Song, B., Zheng, B. & Yu, J. (2018), 'Trim28 protects trim24 from spop-mediated degradation and promotes prostate cancer progression', *Nature communications* **9**(1), 5007.

Fu, M., Wang, C., Reutens, A. T., Wang, J., Angeletti, R. H., Siconolfi-Baez, L., Ogryzko, V., Avantaggiati, M.-L. & Pestell, R. G. (2000), 'p300 and p300/camp-response element-binding protein-associated factor acetylate the androgen receptor at sites governing hormone-dependent transactivation', *Journal of Biological Chemistry* **275**(27), 20853–20860.

Furr, B., Valcaccia, B., Curry, B., Woodburn, J., Chesterson, G. & Tucker, H. (1987), 'Ici 176,334: A novel non–steroidal, peripherally selective antiandrogen', *Journal of Endocrinology* **113**(3), R7–R9.

Georget, V., Lobaccaro, J., Terouanne, B., Mangeat, P., Nicolas, J.-C. & Sultan, C. (1997), 'Trafficking of the androgen receptor in living cells with fused green fluorescent protein–androgen receptor', *Molecular and cellular endocrinology* **129**(1), 17–26.

Giraldo, M. I., Hage, A., van Tol, S. & Rajsbaum, R. (2020), 'Trim proteins in host defense and viral pathogenesis', *Current clinical microbiology reports* **7**(4), 101–114.

Golabek, T., Belsey, J., Drewa, T., Kołodziej, A., Skoneczna, I., Milecki, P., Dobruch, J., Słojewski, M. & Chłosta, P. L. (2016), 'Evidence-based recommendations on androgen deprivation therapy for localized and advanced prostate cancer', *Central European Journal of Urology* **69**(2), 131.

Gravis, G., Audenet, F., Irani, J., Timsit, M.-O., Barthelemy, P., Beuzeboc, P., Fléchon, A., Linassier, C., Oudard, S., Rebillard, X. et al. (2017), 'Chemotherapy in hormone-sensitive metastatic prostate cancer: Evidences and uncertainties from the literature', *Cancer treatment reviews* **55**, 211–217.

Gregory, C. W., Johnson Jr, R. T., Mohler, J. L., French, F. S. & Wilson, E. M. (2001), 'Androgen receptor stabilization in recurrent prostate cancer is associated with hypersensitivity to low androgen', *Cancer research* **61**(7), 2892–2898.

Guenther, M. G., Barak, O. & Lazar, M. A. (2001), 'The smrt and n-cor corepressors are activating cofactors for histone deacetylase 3', *Molecular and cellular biology* **21**(18), 6091–6101.

Hage, A. & Rajsbaum, R. (2019), 'To trim or not to trim: the balance of host–virus interactions mediated by the ubiquitin system', *The Journal of general virology* **100**(12), 1641.

Harris, W. P., Mostaghel, E. A., Nelson, P. S. & Montgomery, B. (2009), 'Androgen deprivation therapy: progress in understanding mechanisms of resistance and optimizing androgen depletion', *Nature clinical practice Urology* **6**(2), 76–85.

Hatakeyama, S. (2017), 'Trim family proteins: roles in autophagy, immunity, and carcinogenesis', *Trends in biochemical sciences* **42**(4), 297–311.

He, B., Kemppainen, J. A., Voegel, J. J., Gronemeyer, H. & Wilson, E. M. (1999), 'Activation function 2 in the human androgen receptor ligand binding domain mediates interdomain communication with the nh2-terminal domain', *Journal of Biological Chemistry* **274**(52), 37219–37225.

Heidtmann, H., Nettelbeck, D., Mingels, A., Jäger, R., Welker, H. & Kontermann, R. (1999), 'Generation of angiostatin-like fragments from plasminogen by prostate-specific antigen', *British journal of cancer* **81**(8), 1269–1273.

Heikel, G., Choudhury, N. & Michlewski, G. (2016), 'The role of Trim25 in development, disease and RNA metabolism', *Biochemical Society Transactions* **44**(4), 1045–1050.

Heinlein, C. A. & Chang, C. (2002), 'Androgen Receptor (AR) Coregulators: An Overview', *Endocrine Reviews* **23**(2), 175–200.

Heinlein, C. A. & Chang, C. (2004), 'Androgen receptor in prostate cancer', *Endocrine reviews* **25**(2), 276–308.

Hodgson, M. C., Astapova, I., Cheng, S., Lee, L. J., Verhoeven, M. C., Choi, E., Balk, S. P. & Hollenberg, A. N. (2005), 'The androgen receptor recruits nuclear receptor corepressor (n-cor) in the presence of mifepristone via its n and c termini revealing a novel molecular mechanism for androgen receptor antagonists', *Journal of Biological Chemistry* **280**(8), 6511–6519.

Horoszewicz, J. S., Leong, S. S., Kawinski, E., Karr, J. P., Rosenthal, H., Chu, T. M., Mirand, E. A. & Murphy, G. P. (1983), 'Lncap model of human prostatic carcinoma', *Cancer research* **43**(4), 1809–1818.

Huang, W., Shostak, Y., Tarr, P., Sawyers, C. & Carey, M. (1999), 'Cooperative assembly of androgen receptor into a nucleoprotein complex that regulates the prostate-specific antigen enhancer', *Journal of Biological Chemistry* **274**(36), 25756–25768.

Huggins, C., Hodges, C. V. et al. (1941), 'Studies on prostatic cancer', *Cancer res* **1**(4), 293–297.

Irvine, R. A., Ma, H., Yu, M. C., Ross, R. K., Stallcup, M. R. & Coetzee, G. A. (2000), 'Inhibition of p160-mediated coactivation with increasing androgen receptor polyglutamine length', *Human Molecular Genetics* **9**(2), 267–274.

Jaworska, A. M., Wlodarczyk, N. A., Mackiewicz, A. & Czerwinska, P. (2020), 'The role of trim family proteins in the regulation of cancer stem cell self-renewal', *Stem Cells* **38**(2), 165–173.

Jha, S. K., Rauniyar, K., Chronowska, E., Mattonet, K., Maina, E. W., Koistinen, H., Stenman, U.-H., Alitalo, K. & Jeltsch, M. (2019), 'Klk3/psa and cathepsin d activate vegf-c and vegf-d', *eLife* **8**, e44478.

Jin, H.-J., Kim, J. & Yu, J. (2013), 'Androgen receptor genomic regulation', *Translational andrology and urology* **2**(3), 158.

Kaku, N., Matsuda, K.-i., Tsujimura, A. & Kawata, M. (2008), 'Characterization of nuclear import of the domain-specific androgen receptor in association with the importin α/β and ran-guanosine 5-triphosphate systems', *Endocrinology* **149**(8), 3960–3969.

Kikuchi, M., Okumura, F., Tsukiyama, T., Watanabe, M., Miyajima, N., Tanaka, J., Imamura, M. & Hatakeyama, S. (2009), 'Trim24 mediates ligand-dependent activation of androgen receptor and is repressed by a bromodomain-containing protein, brd7, in prostate cancer cells', *Biochimica et Biophysica Acta (BBA)-Molecular Cell Research* **1793**(12), 1828–1836.

Koepke, L., Gack, M. U. & Sparrer, K. M. (2021), 'The antiviral activities of trim proteins', *Current opinion in microbiology* **59**, 50–57.

Kolde, R. (2019), 'Pheatmap: Pretty heatmaps, r package version 1.0. 12. 2019'.

Kwon, S. C., Yi, H., Eichelbaum, K., Föhr, S., Fischer, B., You, K. T., Castello, A., Krijgsveld, J., Hentze, M. W. & Kim, V. N. (2013), 'The rna-binding protein repertoire of embryonic stem cells', *Nature structural & molecular biology* **20**(9), 1122–1130.

Lavery, D. & McEwan, I. J. (2006), 'The human androgen receptor af1 transactivation domain: interactions with transcription factor iif and molten-globule-like structural characteristics'.

Leo, C. & Chen, J. D. (2000), 'The src family of nuclear receptor coactivators', *Gene* **245**(1), 1–11.

Li, C., Dou, P., Lu, X., Guan, P., Lin, Z., Zhou, Y., Lu, X., Lin, X. & Xu, G. (2022), 'Identification and validation of trim25 as a glucose metabolism regulator in prostate cancer', *International Journal of Molecular Sciences* **23**(16), 9325.

Lilja, H. et al. (1985), 'A kallikrein-like serine protease in prostatic fluid cleaves the predominant seminal vesicle protein.', *The Journal of clinical investigation* **76**(5), 1899–1903.

Litwin, M. S. & Tan, H.-J. (2017), 'The diagnosis and treatment of prostate cancer: a review', *Jama* **317**(24), 2532–2542.

Liu, Y., Tao, S., Liao, L., Li, Y., Li, H., Li, Z., Lin, L., Wan, X., Yang, X. & Chen, L. (2020), 'Trim25 promotes the cell survival and growth of hepatocellular carcinoma through targeting keap1-nrf2 pathway', *Nature communications* **11**(1), 348.

Love, M., Anders, S. & Huber, W. (2014), 'Differential analysis of count data–the deseq2 package', *Genome Biol* **15**(550), 10–1186.

MacLean, H. E., Warne, G. L. & Zajac, J. D. (1997), 'Localization of functional domains in the androgen receptor', *The Journal of steroid biochemistry and molecular biology* **62**(4), 233–242.

Meroni, G. & Diez-Roux, G. (2005), 'Trim/rbcc, a novel class of 'single protein ring finger' e3 ubiquitin ligases', *BioEssays* **27**(11), 1147–1157.

Moradi, A., Srinivasan, S., Clements, J. & Batra, J. (2019), 'Beyond the biomarker role: Prostate-specific antigen (psa) in the prostate cancer microenvironment', *Cancer and Metastasis Reviews* **38**(3), 333–346.

Mottet, N., Bellmunt, J., Bolla, M., Briers, E., Cumberbatch, M. G., De Santis, M., Fossati, N., Gross, T., Henry, A. M., Joniau, S. et al. (2017), 'Eau-estro-siog guidelines on prostate cancer. part 1: screening, diagnosis, and local treatment with curative intent', *European urology* **71**(4), 618–629.

Nakajima, A., Maruyama, S., Bohgaki, M., Miyajima, N., Tsukiyama, T., Sakuragi, N. & Hatakeyama, S. (2007), 'Ligand-dependent transcription of estrogen receptor α is mediated by the ubiquitin ligase efp', *Biochemical and biophysical research communications* **357**(1), 245–251.

Nakajima, T., Uchida, C., Anderson, S. F., Parvin, J. D. & Montminy, M. (1997), 'Analysis of a camp-responsive activator reveals a two-component mechanism for transcriptional induction via signal-dependent factors.', *Genes & Development* **11**(6), 738–747.

Nakka, M., Agoulnik, I. U. & Weigel, N. L. (2013), 'Targeted disruption of the p160 coactivator interface of androgen receptor (ar) selectively inhibits ar activity in both androgen-dependent and castration-resistant ar-expressing prostate cancer cells', *The international journal of biochemistry & cell biology* **45**(4), 763–772.

National Cancer Institute (2023), 'Prostate cancer prevention (pdq) - health professional version'.
URL: *https://www.cancer.gov/types/prostate/hp/prostate-prevention-pdq*

Nazareth, L. V. & Weigel, N. L. (1996), 'Activation of the human androgen receptor through a protein kinase a signaling pathway', *Journal of Biological Chemistry* **271**(33), 19900–19907.

Nenasheva, V. V. & Tarantul, V. Z. (2020), 'Many faces of trim proteins on the road from pluripotency to neurogenesis', *Stem Cells and Development* **29**(1), 1–14.

Niu, Y., Yeh, S., Miyamoto, H., Li, G., Altuwaijri, S., Yuan, J., Han, R., Ma, T., Kuo, H.-C. & Chang, C. (2008), 'Tissue Prostate-Specific Antigen Facilitates Refractory Prostate Tumor Progression via Enhancing ARA70-Regulated Androgen Receptor Transactivation', *Cancer Research* **68**(17), 7110–7119.

Paliouras, M. & Diamandis, E. P. (2006), 'The kallikrein world: an update on the human tissue kallikreins'.

Pauletto, E., Elabd, S., Eickhoff, N., Padrao, N., Zwart, W. & Blattner, C. (in revision), 'Trim25 targets p300 for degradation'.

Petrera, F. & Meroni, G. (2012), 'Trim proteins in development', *TRIM/RBCC Proteins* pp. 131–141.

Pezzato, E., Sartor, L., Dell'Aica, I., Dittadi, R., Gion, M., Belluco, C., Lise, M. & Garbisa, S. (2004), 'Prostate carcinoma and green tea: Psa-triggered basement membrane degradation and mmp-2 activation are inhibited by ()epigallocatechin-3-gallate', *International Journal of Cancer* **112**(5), 787–792.

Qin, Y., Cui, H. & Zhang, H. (2016), 'Overexpression of trim25 in lung cancer regulates tumor cell progression', *Technology in Cancer Research & Treatment* **15**(5), 707–715.

Quigley, C., Evans, B., Simental, J., Marschke, K., Sar, M., Lubahn, D., Davies, P., Hughes, I., Wilson, E. & French, F. (1992), 'Complete androgen insensitivity due to deletion of exon c of the androgen receptor gene highlights the functional importance of the second zinc finger of the androgen receptor in vivo.', *Molecular endocrinology* **6**(7), 1103–1112.

Reddy, B. A., Etkin, L. D. & Freemont, P. S. (1992), 'A novel zinc finger coiled-coil domain in a family of nuclear proteins', *Trends in biochemical sciences (Amsterdam. Reference ed.)* **17**(9), 344–345.

Reymond, A., Meroni, G., Fantozzi, A., Merla, G., Cairo, S., Luzi, L., Riganelli, D., Zanaria, E., Messali, S., Cainarca, S. et al. (2001), 'The tripartite motif family identifies cell compartments', *The EMBO journal* **20**(9), 2140–2151.

Riegman, P., Vlietstra, R., Van der Korput, J., Brinkmann, A. & Trapman, J. (1991), 'The promoter of the prostate-specific antigen gene contains a functional androgen responsive element', *Molecular endocrinology* **5**(12), 1921–1930.

Ritchie, M. E., Phipson, B., Wu, D., Hu, Y., Law, C. W., Shi, W. & Smyth, G. K. (2015), 'limma powers differential expression analyses for rna-sequencing and microarray studies', *Nucleic acids research* **43**(7), e47–e47.

Robert Koch Institute (2022), 'Prostate cancer statistics', `https://www.krebsdaten.de/Krebs/EN/Content/Cancer_sites/Prostate_cancer/prostate_cancer_node.html`. Accessed: June 1, 2023.

Robinson, J. T., Thorvaldsdóttir, H., Winckler, W., Guttman, M., Lander, E. S., Getz, G. & Mesirov, J. P. (2011), 'Integrative genomics viewer', *Nature biotechnology* **29**(1), 24–26.

Roche, P. J., Hoare, S. A. & Parker, M. G. (1992), 'A consensus dna-binding site for the androgen receptor.', *Molecular endocrinology* **6**(12), 2229–2235.

Rogers, O. C., Anthony, L., Rosen, D. M., Brennen, W. N. & Denmeade, S. R. (2018), 'Psa-selective activation of cytotoxic human serine proteases within the tumor microenvironment as a therapeutic strategy to target prostate cancer', *Oncotarget* **9**(32), 22436.

Ruizeveld de Winter, J., Trapman, J., Vermey, M., Mulder, E., Zegers, N. D. & van der Kwast, T. H. (1991), 'Androgen receptor expression in human tissues: an immunohistochemical study.', *Journal of Histochemistry & Cytochemistry* **39**(7), 927–936.

Rundlett, S. E. & Miesfeld, R. L. (1995), 'Quantitative differences in androgen and glucocorticoid receptor dna binding properties contribute to receptor-selective transcriptional regulation', *Molecular and cellular endocrinology* **109**(1), 1–10.

Réhault, S., Monget, P., Mazerbourg, S., Tremblay, R., Gutman, N., Gauthier, F. & Moreau, T. (2001), 'Insulin-like growth factor binding proteins (igfbps) as potential physiological substrates for human kallikreins hk2 and hk3', *European Journal of Biochemistry* **268**(10), 2960–2968.

Saha, S., Panigrahi, D. P., Patil, S. & Bhutia, S. K. (2018), 'Autophagy in health and disease: A comprehensive review', *Biomedicine & Pharmacotherapy* **104**, 485–495.

Sakuma, M., Akahira, J.-i., Suzuki, T., Inoue, S., Ito, K., Moriya, T., Sasano, H., Okamura, K. & Yaegashi, N. (2005), 'Expression of estrogen-responsive finger protein (efp) is associated with advanced disease in human epithelial ovarian cancer', *Gynecologic oncology* **99**(3), 664–670.

Sandhu, S., Moore, C., Chiong, E., Beltran, H., Bristow, R. & Williams, S. (2021), 'Prostate cancer', *The Lancet* **398**(10305), 1075–1090.

Scher, H. I., Beer, T. M., Higano, C. S., Anand, A., Taplin, M.-E., Efstathiou, E., Rathkopf, D., Shelkey, J., Evan, Y. Y., Alumkal, J. et al. (2010), 'Antitumour activity of mdv3100 in castration-resistant prostate cancer: a phase 1–2 study', *The Lancet* **375**(9724), 1437–1446.

Scher, H. I., Fizazi, K., Saad, F., Taplin, M.-E., Sternberg, C. N., Miller, K., De Wit, R., Mulders, P., Chi, K. N., Shore, N. D. et al. (2012), 'Increased survival with enzalutamide in prostate cancer after chemotherapy', *New England Journal of Medicine* **367**(13), 1187–1197.

Schuur, E. R., Henderson, G. A., Kmetec, L. A., Miller, J. D., Lamparski, H. G. & Henderson, D. R. (1996), 'Prostate-specific antigen expression is regulated by an upstream enhancer ()', *Journal of Biological Chemistry* **271**(12), 7043–7051.

Shang, Y., Myers, M. & Brown, M. (2002), 'Formation of the androgen receptor transcription complex', *Molecular cell* **9**(3), 601–610.

Sharifi, N. (2013), 'Minireview: androgen metabolism in castration-resistant prostate cancer', *Molecular endocrinology* **27**(5), 708–714.

Shim, M. & Cohen, P. (1999), 'Igfs and human cancer: implications regarding the risk of growth hormone therapy', *Hormone Research in Paediatrics* **51**(Suppl. 3), 42–51.

Shukla, G., Plaga, A., Shankar, E. & Gupta, S. (2016), 'Androgen receptor-related diseases: what do we know?', *Andrology* **4**(3), 366–381.

Spencer, T. E., Jenster, G., Burcin, M. M., Allis, C. D., Zhou, J., Mizzen, C. A., McKenna, N. J., Onate, S. A., Tsai, S. Y., Tsai, M.-J. et al. (1997), 'Steroid receptor coactivator-1 is a histone acetyltransferase', *Nature* **389**(6647), 194–198.

Stenman, U.-H., Leinonen, J., Zhang, W.-M., Finne, P. & Wu, P. (1998), 'The clinical importance of free prostate-specific antigen (psa)', *Current opinion in urology* **8**(5), 393–399.

Subramanian, A., Tamayo, P., Mootha, V. K., Mukherjee, S., Ebert, B. L., Gillette, M. A., Paulovich, A., Pomeroy, S. L., Golub, T. R., Lander, E. S. et al. (2005), 'Gene set enrichment analysis: a knowledge-based approach for interpreting genome-wide expression profiles', *Proceedings of the National Academy of Sciences* **102**(43), 15545–15550.

Sung, H., Ferlay, J., Siegel, R. L., Laversanne, M., Soerjomataram, I., Jemal, A. & Bray, F. (2021), 'Global cancer statistics 2020: Globocan estimates of incidence and mortality worldwide for 36 cancers in 185 countries', *CA: A Cancer Journal for Clinicians* **71**(3), 209–249.

Takayama, K.-i., Suzuki, T., Tanaka, T., Fujimura, T., Takahashi, S., Urano, T., Ikeda, K. & Inoue, S. (2018), 'Trim25 enhances cell growth and cell survival by modulating p53 signals via interaction with g3bp2 in prostate cancer', *Oncogene* **37**(16), 2165–2180.

Tan, E., Li, J., Xu, H. E., Melcher, K. & leong Yong, E. (2014), 'Androgen receptor: structure, role in prostate cancer and drug discovery', *Acta Pharmacologica Sinica* **36**(36), 3–23.

Tannock, I. F., De Wit, R., Berry, W. R., Horti, J., Pluzanska, A., Chi, K. N., Oudard, S., Théodore, C., James, N. D., Turesson, I. et al. (2004), 'Docetaxel plus prednisone or mitoxantrone plus prednisone for advanced prostate cancer', *New England Journal of Medicine* **351**(15), 1502–1512.

Tomlins, S. A., Rhodes, D. R., Perner, S., Dhanasekaran, S. M., Mehra, R., Sun, X.-W., Varambally, S., Cao, X., Tchinda, J., Kuefer, R. et al. (2005), 'Recurrent fusion of tmprss2 and ets transcription factor genes in prostate cancer', *science* **310**(5748), 644–648.

Tran, C., Ouk, S., Clegg, N. J., Chen, Y., Watson, P. A., Arora, V., Wongvipat, J., Smith-Jones, P. M., Yoo, D., Kwon, A. et al. (2009), 'Development of a second-generation antiandrogen for treatment of advanced prostate cancer', *Science* **324**(5928), 787–790.

Ueda, T., Mawji, N. R., Bruchovsky, N. & Sadar, M. D. (2002), 'Ligand-independent activation of the androgen receptor by interleukin-6 and the role of steroid receptor coactivator-1 in prostate cancer cells', *Journal of Biological Chemistry* **277**(41), 38087–38094.

Uhlen, M., Zhang, C., Lee, S., Sjöstedt, E., Fagerberg, L., Bidkhori, G., Benfeitas, R., Arif, M., Liu, Z., Edfors, F. et al. (2017), 'A pathology atlas of the human cancer transcriptome', *Science* **357**(6352), eaan2507.

Urano, T., Saito, T., Tsukui, T., Fujita, M., Hosoi, T., Muramatsu, M., Ouchi, Y. & Inoue, S. (2002), 'Efp targets 14-3-3σ for proteolysis and promotes breast tumour growth', *Nature* **417**(6891), 871–875.

van Gent, M., Sparrer, K. M. & Gack, M. U. (2018), 'Trim proteins and their roles in antiviral host defenses', *Annual review of virology* **5**(1), 385.

Venuto, S. & Merla, G. (2019), 'E3 ubiquitin ligase trim proteins, cell cycle and mitosis', *Cells* **8**(5), 510.

Veveris-Lowe, T., Lawrence, M., Collard, R., Bui, L., Herington, A., Nicol, D. & Clements, J. (2005), 'Kallikrein 4 (hk4) and prostate-specific antigen (psa) are associated with the loss of e-cadherin and an epithelial-mesenchymal

transition (emt)-like effect in prostate cancer cells', *Endocrine Related Cancer* **12**(3), 631–644.

Visakorpi, T., Hyytinen, E., Koivisto, P., Tanner, M., Keinänen, R., Palmberg, C., Palotie, A., Tammela, T., Isola, J. & Kallioniemi, O.-P. (1995), 'In vivo amplification of the androgen receptor gene and progression of human prostate cancer', *Nature genetics* **9**(4), 401–406.

Walsh, L. A., Alvarez, M. J., Sabio, E. Y., Reyngold, M., Makarov, V., Mukherjee, S., Lee, K.-W., Desrichard, A., Turcan, Ş., Dalin, M. G. et al. (2017), 'An integrated systems biology approach identifies trim25 as a key determinant of breast cancer metastasis', *Cell reports* **20**(7), 1623–1640.

Wang, Q., Li, W., Zhang, Y., Yuan, X., Xu, K., Yu, J., Chen, Z., Beroukhim, R., Wang, H., Lupien, M. et al. (2009), 'Androgen receptor regulates a distinct transcription program in androgen-independent prostate cancer', *Cell* **138**(2), 245–256.

Wang, S., Kollipara, R. K., Humphries, C. G., Ma, S.-H., Hutchinson, R., Li, R., Siddiqui, J., Tomlins, S. A., Raj, G. V. & Kittler, R. (2016), 'The ubiquitin ligase trim25 targets erg for degradation in prostate cancer', *Oncotarget* **7**(40), 64921.

Webber, M. M., Waghray, A. & Bello, D. (1995), 'Prostate-specific antigen, a serine protease, facilitates human prostate cancer cell invasion.', *Clinical cancer research: an official journal of the American Association for Cancer Research* **1**(10), 1089–1094.

Weinert, C., Morger, D., Djekic, A., Grütter, M. G. & Mittl, P. R. (2015), 'Crystal structure of trim20 c-terminal coiled-coil/b30. 2 fragment: implications for the recognition of higher order oligomers', *Scientific reports* **5**(1), 1–10.

Welti, J., Sharp, A., Brooks, N., Yuan, W., McNair, C., Chand, S. N., Pal, A., Figueiredo, I., Riisnaes, R., Gurel, B. et al. (2021), 'Targeting the p300/cbp axis in lethal prostate cancer', *Cancer Discovery* **11**(5), 1118–1137.

Wickham, H. (2016), *ggplot2: Elegant Graphics for Data Analysis*, Springer-Verlag New York.

Wilbert, D. M., GRIFFIN, J. E. & Wilson, J. D. (1983), 'Characterization of the cytosol androgen receptor of the human prostate', *The Journal of Clinical Endocrinology & Metabolism* **56**(1), 113–120.

Wu, T., Hu, E., Xu, S., Chen, M., Guo, P., Dai, Z., Feng, T., Zhou, L., Tang, W., Zhan, L. et al. (2021), 'clusterprofiler 4.0: A universal enrichment tool for interpreting omics data', *The Innovation* **2**(3), 100141.

Xu, Y., Chen, S. & Balk, S. P. (2006), Androgen receptor signaling induces prostate cancer cell proliferation through mtor activation and post-transcriptional increases in cyclin d proteins, *in* 'CANCER RESEARCH', Vol. 66.

Yang, E., Huang, S., Jami-Alahmadi, Y., McInerney, G. M., Wohlschlegel, J. A. & Li, M. M. (2022), 'Elucidation of trim25 ubiquitination targets involved in diverse cellular and antiviral processes', *PLoS Pathogens* **18**(9), e1010743.

Yu, X., Yi, P., Hamilton, R. A., Shen, H., Chen, M., Foulds, C. E., Mancini, M. A., Ludtke, S. J., Wang, Z. & O'Malley, B. W. (2020), 'Structural insights of transcriptionally active, full-length androgen receptor coactivator complexes', *Molecular cell* **79**(5), 812–823.

Zhang, L., Afolabi, L. O., Wan, X., Li, Y. & Chen, L. (2020), 'Emerging roles of tripartite motif-containing family proteins (trims) in eliminating misfolded proteins', *Frontiers in Cell and Developmental Biology* **8**, 802.

Zhang, P., Elabd, S., Hammer, S., Solozobova, V., Yan, H., Bartel, F., Inoue, S., Henrich, T., Wittbrodt, J., Loosli, F. et al. (2015), 'Trim25 has a dual function in the p53/mdm2 circuit', *Oncogene* **34**(46), 5729–5738.

Zhong, J., Ding, L., Bohrer, L. R., Pan, Y., Liu, P., Zhang, J., Sebo, T. J., Karnes, R. J., Tindall, D. J., Van Deursen, J. et al. (2014), 'p300 acetyltransferase regulates androgen receptor degradation and pten-deficient prostate tumorigenesisp300 regulates ar degradation and prostate tumorigenesis', *Cancer research* **74**(6), 1870–1880.

Zhu, S., Gu, H., Peng, C., Xia, F., Cao, H. & Cui, H. (2022), 'Regulation of glucose, fatty acid and amino acid metabolism by ubiquitination and sumoylation for cancer progression.', *Frontiers in Cell and Developmental Biology* p. 581.